BEILSTEIN JOURNAL OF ORGANIC CHEMISTRY

Late-stage diversification of peptides

Edited by Norbert Sewald

Generated on 06 November 2026, 18:41

Imprint

Beilstein Journal of Organic Chemistry
www.bjoc.org
ISSN 1860-5397
Email: journals-support@beilstein-institut.de

The *Beilstein Journal of Organic Chemistry* is published by the Beilstein-Institut zur Förderung der Chemischen Wissenschaften.

Beilstein-Institut zur Förderung der Chemischen Wissenschaften
Trakehner Straße 7–9
60487 Frankfurt am Main
Germany
www.beilstein-institut.de

The copyright to this document as a whole, which is published in the *Beilstein Journal of Organic Chemistry*, is held by the Beilstein-Institut zur Förderung der Chemischen Wissenschaften. The copyright to the individual articles in this document is held by the respective authors, subject to a Creative Commons Attribution license.

BEILSTEIN JOURNAL OF ORGANIC CHEMISTRY

A photochemical C=C cleavage process: toward access to backbone *N*-formyl peptides

Haopei Wang and Zachary T. Ball*

Letter

Open Access

Address:
Department of Chemistry, Rice University, Houston TX, USA

Email:
Zachary T. Ball* - zach.ball@gmail.com

* Corresponding author

Keywords:
formyl peptide; nitroaryl compound; nitroso compound; olefin cleavage; photocleavage

Beilstein J. Org. Chem. **2021,** *17,* 2932–2938.
https://doi.org/10.3762/bjoc.17.202

Received: 11 October 2021
Accepted: 30 November 2021
Published: 15 December 2021

This article is part of the thematic issue "Late-stage diversification of peptides".

Associate Editor: N. Sewald

© 2021 Wang and Ball; licensee Beilstein-Institut.
License and terms: see end of document.

Abstract

Photo-responsive modifications and photo-uncaging concepts are useful for spatiotemporal control of peptides structure and function. While side chain photo-responsive modifications are relatively common, access to photo-responsive modifications of backbone N–H bonds is quite limited. This letter describes a new photocleavage pathway, affording *N*-formyl amides from vinylogous nitroaryl precursors under physiologically relevant conditions via a formal oxidative C=C cleavage. The *N*-formyl amide products have unique properties and reactivity, but are difficult or impossible to access by traditional synthetic approaches.

Findings

The photochemistry of nitroaromatic functional groups has a rich history that dates back decades [1-5]. Photochemical pathways allow access to diverse and interesting target structures [6-10], though photocleavage of C–X bonds for use as photoremovable protecting groups [11,12] has been the major thrust of the development of 2-nitroaryl compounds. Various 2-nitrobenzyl derivatives are used to photocage heteroatom functional groups, including alcohols, amines, carboxylic acids, and phosphates [11]. Typical photochemical pathways result in cleavage of a benzylic C–X bond following initial benzylic H-atom abstraction [11,13]. In contrast, photorelease systems based on C–C or C=C bond photocleavage are quite rare [14,15]. We recently reported a vinylogous analogue of this photo-deprotection process, which allowed photocleavage of alkenyl sp^2 C–X bonds, rather than benzylic sp^3 C–X cleavage [16,17]. We now report that further studies into this reaction demonstrate two mechanistically distinct photocleavage pathways, with selectivity dependent on pH. In addition to an anticipated alkenyl sp^2 C–X bond cleavage pathway, we identified a new photochemical reaction pathway, prevalent under neutral and acidic reaction conditions, which leads to formyl products from formal oxidative cleavage of a C=C bond.

Our interest in vinylogous analogues of 2-nitroaryl photoreactive groups stems from studies into alkenylboronic acid reagents for Chan–Lam-type modification of peptide backbone N–H bonds, directed by a proximal histidine residue (Figure 1C, step, **i** + **iv** → **ii**) [18-20]. Subsequent investigations validated the use of photoreactive boronic acids as an approach to reversible backbone N–H modification via photocleavage of an alkenyl C–N bond [16,17]. Traditional 2-nitroaryl groups allow cleavage of benzylic C–X bonds (e.g. C–O cleavage, Figure 1A) through H-atom abstraction from a photoexcited intermediate, which produces an oxonium-type intermediate (in brackets). Hydrolysis of this intermediate then affords an alcohol product. Recently [16,17], we demonstrated that vinylogous analogues of this mechanism (Figure 1B) provide entry into similar photouncaging chemistries for amide release.

Figure 1C shows an example of this concept applied to a peptide substrate. Reaction of the peptide **i** with an alkenyl-

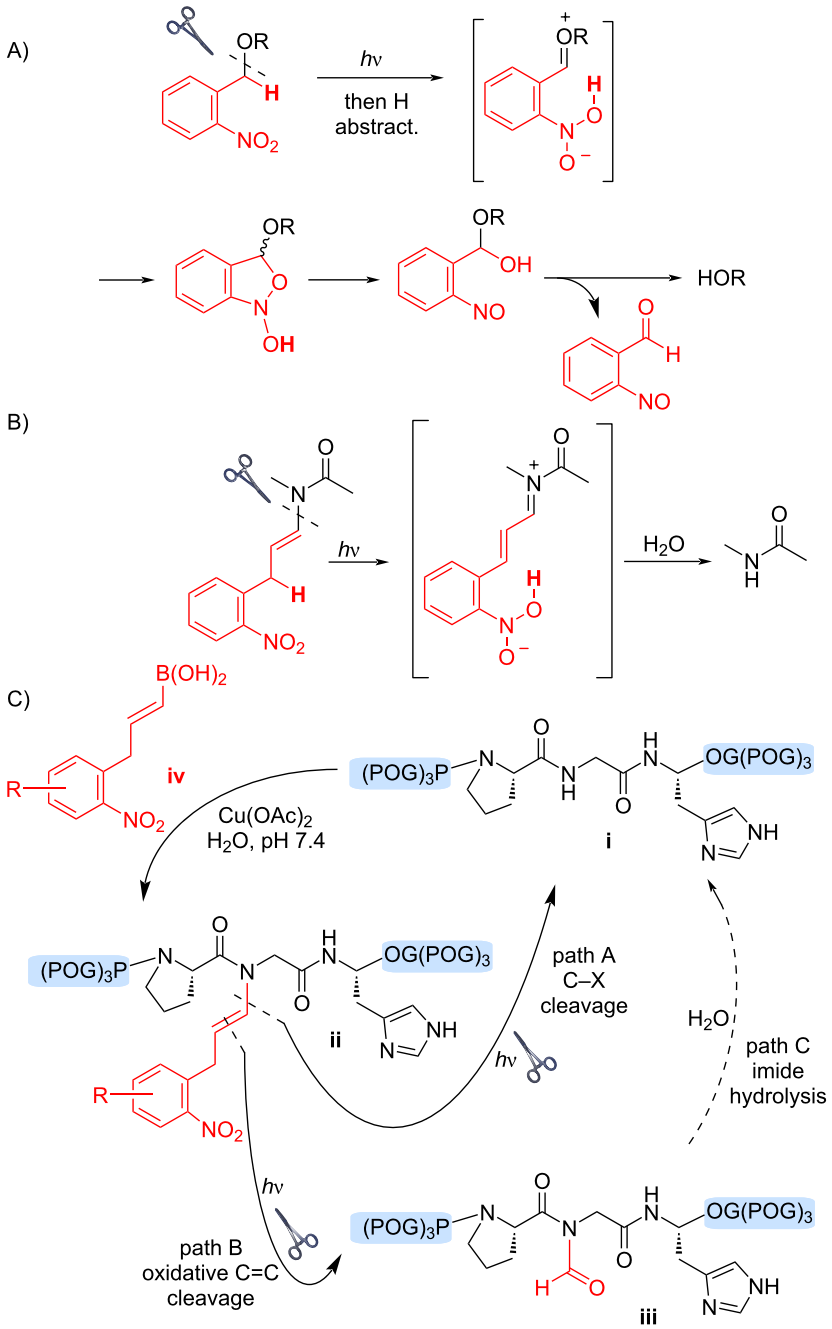


Figure 1: Uncaging of peptide backbone N–H bonds from Chan–Lam-type modification.

boronic acid reagent **iv** in the presence of a copper(II) salt in water provides access to the backbone N–H alkenylation product **ii**, directed by a neighboring histidine residue. Upon exposure to 365-nm light, photocleavage of the caging group (red) was observed, producing the free peptide **i**. Irradiation longer than 10 minutes were sometimes necessary for maximal yield of photo-deprotected product **i** [16]. Furthermore, byproducts or transiently stable intermediates were sometimes indicated by HPLC and/or NMR of these photocleavage reactions [16,17]. These observations prompted a more detailed study of the components present during photocleavage reactions of small-molecule models, leading to the identification of the *N*-formyl product **iii**, a possible intermediate on the path to product **i** via imide hydrolysis.

To better understand the mechanism of photocleavage and the appearance of the formyl product **iii**, we first identified the 2-nitroaryl-derived byproducts produced in this reaction. Model compound **1** was subjected to aqueous photocleavage in the presence of triethylamine, and the resulting reaction mixture was purified by reversed-phase HPLC (Figure 2). We isolated a nitroso product **3**, in addition to two other major identifiable components of the crude reaction: quinoline *N*-oxide (**4**) and quinolinone (**5**). The compounds **4** and **5** are C_9 compounds possibly derived from thermal or photochemical rearrangement of compound **3** or another intermediate. The yield of each product was calculated by NMR and verified by isolation (Figure 2). To test the generality of this process with other functional groups, we prepared and tested alkenyl ether **6** as a model of C–O-bond cleavage. Photoirradiation of the ether **6** similarly provided a mixture of C_9-containing products **3**, **4**, and **5**. Under these reaction conditions, the C–X cleavage products (MeOH or **2**) were observed, but no formyl products were formed. The C_9 byproducts – the nitroso **3**, and related compounds **4** and **5** are all consistent with the classical C–X cleavage mechanism and with hydrolysis of the presumed oxonium intermediate **6'**, but are inconsistent with the production of formyl products.

In contrast, photoirradiation of the same alkenyl ether **6** under acidic conditions at pH 4.0 provided a mixture of methanol (53%) and methyl formate (38%, **7**) as determined by NMR, the latter product is the result of formal oxidative C=C cleavage (Figure 3a). Alkenyl amide **1** at pH 4.0 similarly gave mixtures of the C–N cleavage product **2** and C=C cleavage product **8**. We examined product selectivity in the irradiation of alkenyl amide **1** across a range of pH and found a significant correlation (Figure 3b–d). The formyl product **8** predominated at acidic and neutral pH. The amount of **8** decreased with increasing pH, and above pH 10 the C–X cleavage product **2** became the major product. Unfortunately, no products other than the formyl compound were isolated after photocleavage of compound **1** or **6** in acidic conditions. Instead, when irradiation of alkenyl amide **1** was conducted in acetone, crude NMR analysis indicated the appearance of product **8** as well as new peaks in the aromatic region.

Following acetylation of the reaction mixture, we were able to isolate small quantities of *O*-acetyl *N*-hydroxyindole (**9**,

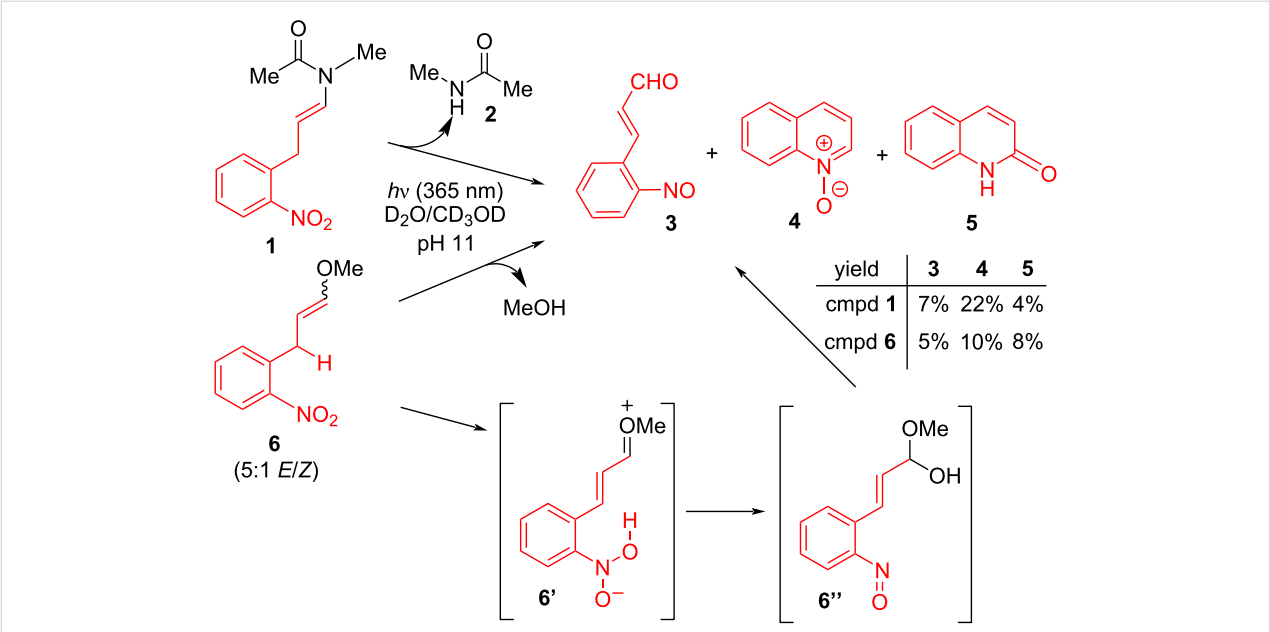


Figure 2: Photocleavage of compounds **1** and **6** under basic conditions. Yield of products was calculated from crude ^{1}H NMR using residual CD_3OD peaks as internal standard.

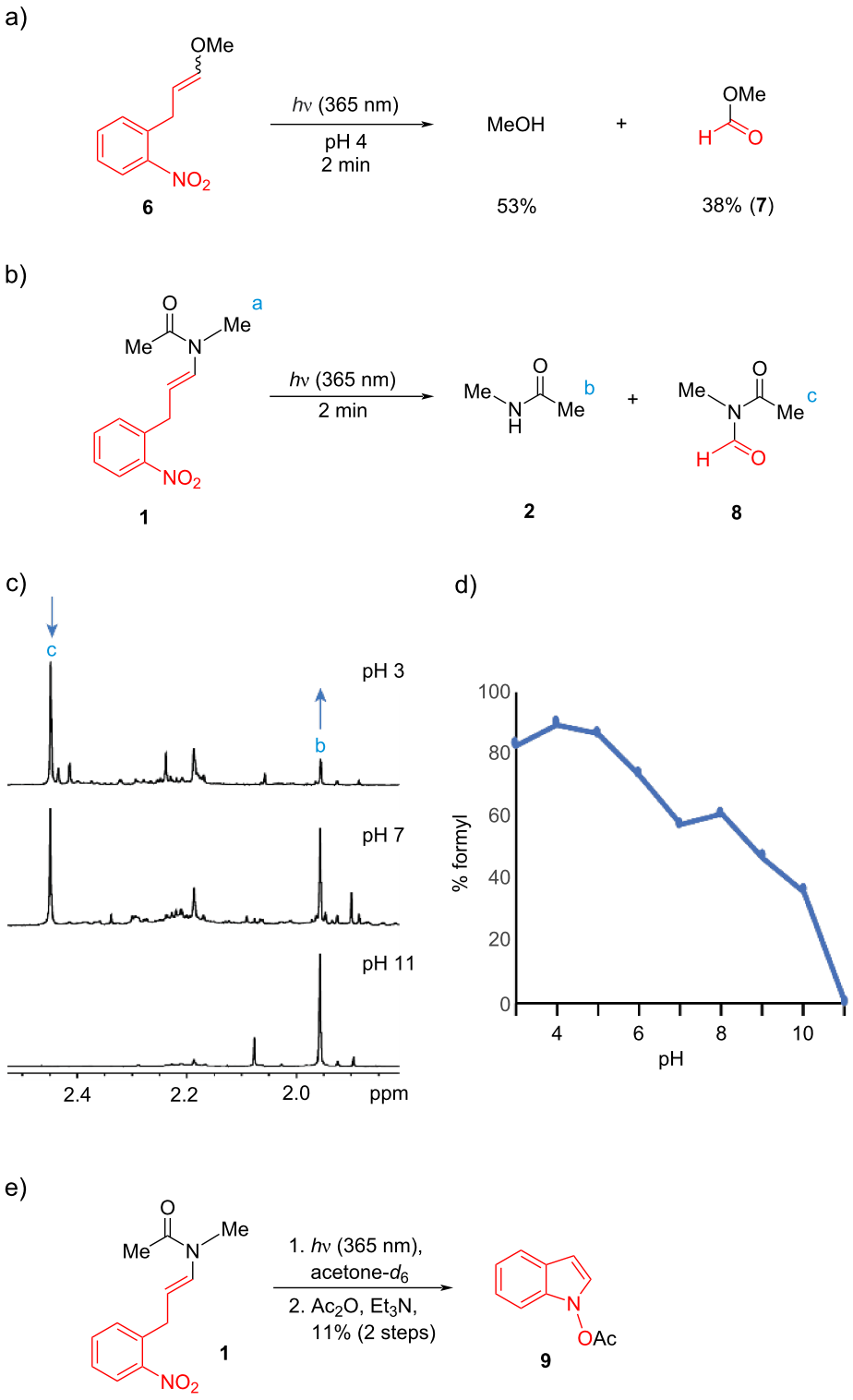


Figure 3: (a) Photocleavage of compound **6** under acidic conditions. Yields determined by ^{1}H NMR using residual CD_3OD as an internal standard. (b–d) Selectivity of photocleavage of alkenyl amide **1** as a function of pH. Product percentage of *N*-formyl **8** was assessed by crude NMR (c) and graphed (d). Formation of *N*-formyl-*N*-methyl acetamide **8** during photocleavage of compound **1**. Conditions: **1** (1.8 μmol) was dissolved in MeOD-d_4 (200 μL) and deuterated buffer (400 μL). The solution was irradiated at 365 nm for 2 min. (e) Photocleavage reaction of **1** in acetone.

Figure 3e), although the initial byproduct *N*-hydroxyindole itself proved too unstable to be isolated. It is noteworthy within this context that hydroxyindole is a C_8 compound, consistent with transfer of the C_1 formyl group to compound **8**. The formation of amide **2** at elevated pH could, in theory, derive from hydrolysis of the initially formed formyl product **8** (i.e. Figure 1C). However, the appearance of primarily C_9 byproducts in the formation of amide **2** at elevated pH precludes pathways involving the intermediacy of **8**. To provide additional support for this analysis, and to assess the stability of *N*-formyl amides formed in this reaction, we irradiated alkenyl amide **10**, which contains a 2-phenylethyl substituent that allowed easier isolation of *N*-formyl **11** (Figure 4). After irradiation, the product **11** was isolated in 28% yield, the modest yield reflecting the instability in water and on silica of this compound. The purified *N*-formyl **11** was then dissolved in buffer (pH 8), and its hydrolysis to amide **12** was assessed (Figure 4, inset). We observed clean first-order kinetics to give amide **12** with a half-life ($t_{1/2}$) of 6.4 h.

The observation of *N*-formyl products can be rationalized with a bifurcating mechanism (Figure 5). Following photoactivation, H-atom abstraction and nucleophilic addition of water would produce the key intermediate **B**. Such hemi-aminal compounds would be unstable under basic conditions, readily forming aldehyde products **3**. However, related hemi-aminal compounds are quite stable under non-basic conditions, and the motif is even contained in some natural products, such as zampanolide [21] and spergualin [22]. We propose a competing electrocyclization pathway, affording the heterocycle **D**, a pathway which should not be base-catalyzed, and thus may be reasonably predominant under appropriate conditions. From heterocycle **D**, a C–C cleavage would produce the *N*-formyl product **8** and a re-aromatized C_8 heterocyclic byproduct **E**. Rearrangement to hydroxyindole (**F**) would then account for the isolation of the acetylated analogue **9**.

The photochemical pathway described here represents a formal oxidative olefin cleavage of vinylogous nitroaryl-modified amides and ethers. The pathway adds to the diversity of photochemical pathways known for 2-nitrophenyl systems, and the concept described here might be useful for the synthetic unmasking of relatively sensitive imido structures. For chemical biology applications, the results point to a far more diverse photochemistry than previously assumed for vinylogous photocleavage systems. Although formyl hydrolysis to the "expected" amide products can and does occur under physiological conditions, the rates of this hydrolysis are slow for the simple models in this study. Within more complex peptides or proteins, selectivity in photocleavage pathways may differ significantly, depending on local chemical environment. It is also worth noting that *N*-formyl products are themselves acylating reagents, and thus could find use in photochemical generation of selective acyl donors.

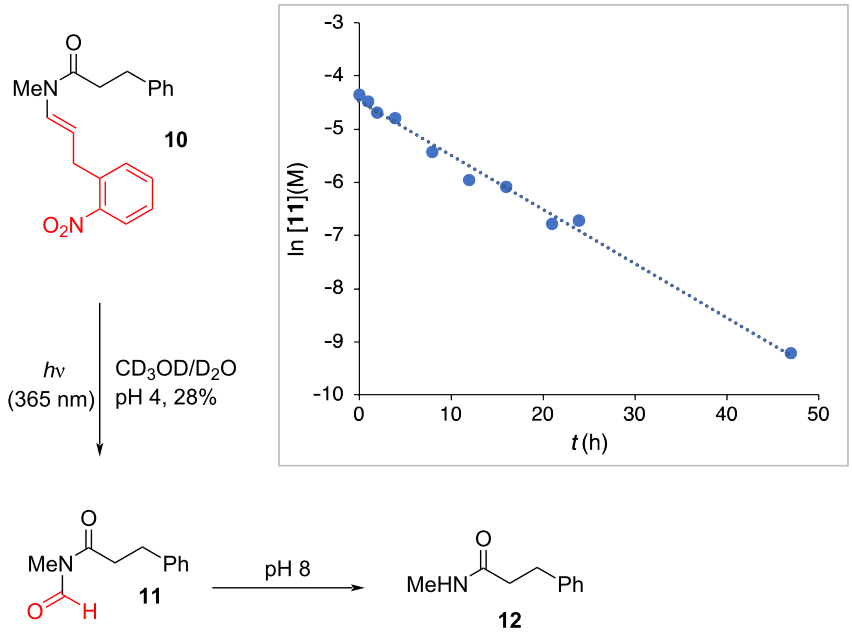


Figure 4: Preparation and hydrolysis kinetics (inset) of *N*-formyl product **11**. Dashed line: first-order decay fit used in calculating the rate constant.

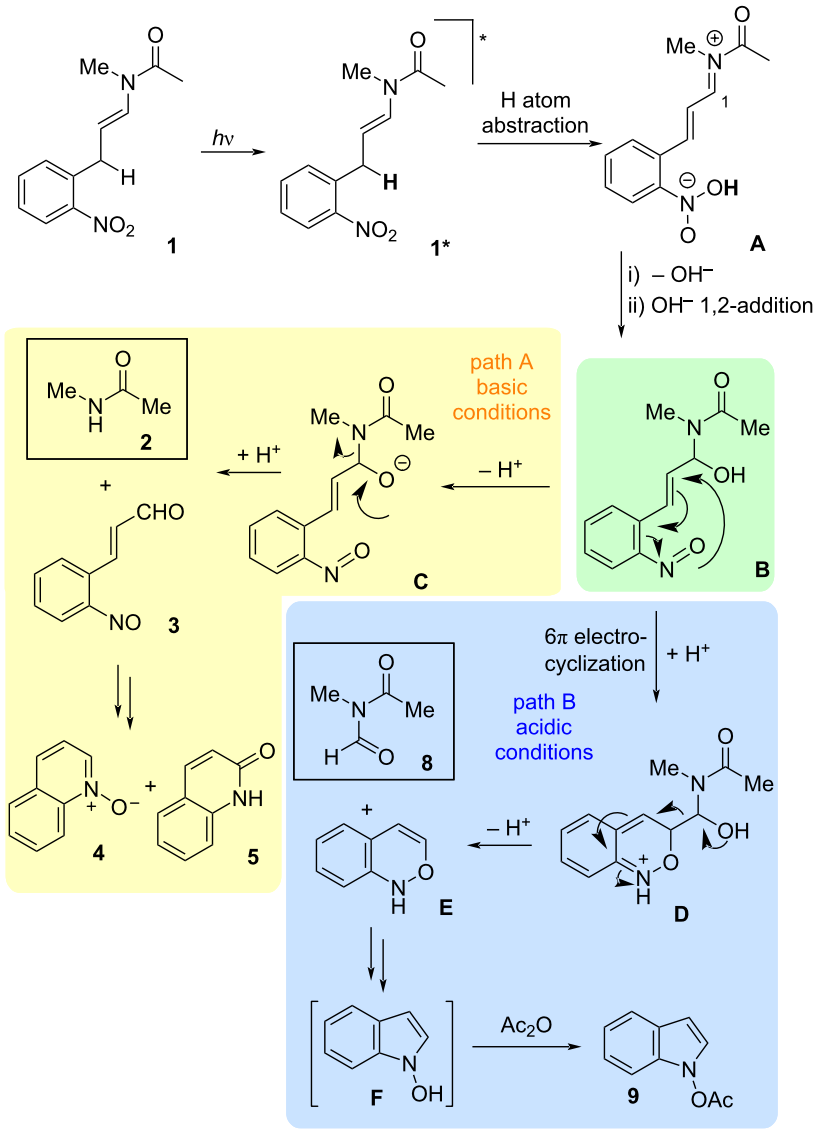


Figure 5: Proposed mechanism for the formation of aldehyde **3** and *N*-formyl product **8**.

Supporting Information

Supporting Information File 1

Experimental section and additional information.
[https://www.beilstein-journals.org/bjoc/content/supplementary/1860-5397-17-202-S1.pdf]

Funding

We acknowledge support from the Robert A. Welch Foundation Research Grant C-1680 (Z.T.B.), and the National Science Foundation under grant number CHE-1904865.

ORCID® iDs

Haopei Wang - https://orcid.org/0000-0001-9756-8783
Zachary T. Ball - https://orcid.org/0000-0002-8681-0789

References

1. Jones, L. B.; Kudrna, J. C.; Foster, J. P. *Tetrahedron Lett.* **1969,** *10,* 3263–3265. doi:10.1016/s0040-4039(01)88404-5
2. Barltrop, J. A.; Bunce, N. J. *J. Chem. Soc. C* **1968,** 1467–1474. doi:10.1039/j39680001467
3. Finnegan, R. A.; Knutson, D. *J. Am. Chem. Soc.* **1968,** *90,* 1670–1671. doi:10.1021/ja01008a061
4. Hamanoue, K.; Amano, M.; Kimoto, M.; Kajiwara, Y.; Nakayama, T.; Teranishi, H. *J. Am. Chem. Soc.* **1984,** *106,* 5993–5997. doi:10.1021/ja00332a041

5. Chapman, O. L.; Heckert, D. C.; Reasoner, J. W.; Thackaberry, S. P. *J. Am. Chem. Soc.* **1966,** *88,* 5550–5554. doi:10.1021/ja00975a037
6. Bellingund, K.; Mathew, T.; Hunt, J. R.; Nirmalchandar, A.; Haiges, R.; Dawlaty, J.; Prakash, G. K. S. *J. Am. Chem. Soc.* **2019,** *141,* 15921–15931. doi:10.1021/jacs.9b07241
7. Nie, H.-J.; Guo, A.-D.; Lin, H.-X.; Chen, X.-H. *RSC Adv.* **2019,** *9,* 13249–13253. doi:10.1039/c9ra02466b
8. Zhu, J. S.; Kraemer, N.; Li, C. J.; Haddadin, M. J.; Kurth, M. J. *J. Org. Chem.* **2018,** *83,* 15493–15498. doi:10.1021/acs.joc.8b02356
9. Guo, A.-D.; Wei, D.; Nie, H.-J.; Hu, H.; Peng, C.; Li, S.-T.; Yan, K.-N.; Zhou, B.-S.; Feng, L.; Fang, C.; Tan, M.; Huang, R.; Chen, X.-H. *Nat. Commun.* **2020,** *11,* 5472. doi:10.1038/s41467-020-19274-y
10. Charlton, J. L.; Liao, C. C.; De Mayo, P. *J. Am. Chem. Soc.* **1971,** *93,* 2463–2471. doi:10.1021/ja00739a018
11. Klán, P.; Šolomek, T.; Bochet, C. G.; Blanc, A.; Givens, R.; Rubina, M.; Popik, V.; Kostikov, A.; Wirz, J. *Chem. Rev.* **2013,** *113,* 119–191. doi:10.1021/cr300177k
12. Pelliccioli, A. P.; Wirz, J. *Photochem. Photobiol. Sci.* **2002,** *1,* 441–458. doi:10.1039/b200777k
13. Gaplovsky, M.; Il'ichev, Y. V.; Kamdzhilov, Y.; Kombarova, S. V.; Mac, M.; Schwörer, M. A.; Wirz, J. *Photochem. Photobiol. Sci.* **2005,** *4,* 33–42. doi:10.1039/b409927c
14. Ichinose, N.; Mizuno, K.; Otsuji, Y.; Caldwell, R. A.; Helms, A. M. *J. Org. Chem.* **1998,** *63,* 3176–3184. doi:10.1021/jo971111s
15. Sako, M.; Shimada, K.; Hirota, K.; Maki, Y. *Tetrahedron Lett.* **1986,** *27,* 3877–3880. doi:10.1016/s0040-4039(00)83904-0
16. Mangubat-Medina, A. E.; Martin, S. C.; Hanaya, K.; Ball, Z. T. *J. Am. Chem. Soc.* **2018,** *140,* 8401–8404. doi:10.1021/jacs.8b04893
17. Mangubat-Medina, A. E.; Trial, H. O.; Vargas, R. D.; Setegne, M. T.; Bader, T.; Distefano, M. D.; Ball, Z. T. *Org. Biomol. Chem.* **2020,** *18,* 5110–5114. doi:10.1039/d0ob00923g
18. Ohata, J.; Minus, M. B.; Abernathy, M. E.; Ball, Z. T. *J. Am. Chem. Soc.* **2016,** *138,* 7472–7475. doi:10.1021/jacs.6b03390
19. Ohata, J.; Zeng, Y.; Segatori, L.; Ball, Z. T. *Angew. Chem., Int. Ed.* **2018,** *57,* 4015–4019. doi:10.1002/anie.201800828
20. Hanaya, K.; Miller, M. K.; Ball, Z. T. *Org. Lett.* **2019,** *21,* 2445–2448. doi:10.1021/acs.orglett.9b00759
21. Troast, D. M.; Porco, J. A. *Org. Lett.* **2002,** *4,* 991–994. doi:10.1021/ol025558l
22. Kondo, S.; Iwasawa, H.; Ikeda, D.; Umeda, Y.; Ikeda, Y.; Iinuma, H.; Umezawa, H. *J. Antibiot.* **1981,** *34,* 1625–1627. doi:10.7164/antibiotics.34.1625

License and Terms

This is an open access article licensed under the terms of the Beilstein-Institut Open Access License Agreement (https://www.beilstein-journals.org/bjoc/terms), which is identical to the Creative Commons Attribution 4.0 International License (https://creativecommons.org/licenses/by/4.0). The reuse of material under this license requires that the author(s), source and license are credited. Third-party material in this article could be subject to other licenses (typically indicated in the credit line), and in this case, users are required to obtain permission from the license holder to reuse the material.

The definitive version of this article is the electronic one which can be found at:
https://doi.org/10.3762/bjoc.17.202

BEILSTEIN JOURNAL OF ORGANIC CHEMISTRY

Peptide stapling by late-stage Suzuki–Miyaura cross-coupling

Hendrik Gruß[1], Rebecca C. Feiner[‡2], Ridhiwan Mseya[‡3], David C. Schröder[1], Michał Jewgiński[4], Kristian M. Müller[2], Rafał Latajka[4], Antoine Marion[*3] and Norbert Sewald[*1]

Full Research Paper

Open Access

Address:
[1]Department of Chemistry, Bielefeld University, Universitätsstr. 25, 33615 Bielefeld, Germany, [2]Department of Technology, Bielefeld University, Universitätsstr. 25, 33615 Bielefeld, Germany, [3]Department of Chemistry, Middle East Technical University, 06800, Ankara, Turkey and [4]Department of Bioorganic Chemistry, Wrocław University of Science and Technology, Wybrzeze Wyspianskiego 27, 50-370 Wrocław, Poland

Email:
Antoine Marion[*] - amarion@metu.edu.tr; Norbert Sewald[*] - norbert.sewald@uni-bielefeld.de

* Corresponding author ‡ Equal contributors

Keywords:
accelerated molecular dynamics; halotryptophan; intrinsically disordered peptides; late-stage diversification; macrocyclisation; molecular dynamics; stapled peptides; Suzuki–Miyaura cross-coupling

Beilstein J. Org. Chem. **2022,** *18,* 1–12.
https://doi.org/10.3762/bjoc.18.1

Received: 09 July 2021
Accepted: 09 December 2021
Published: 03 January 2022

This article is part of the thematic issue "Late-stage diversification of peptides".

Associate Editor: K. N. Allen

© 2022 Gruß et al.; licensee Beilstein-Institut.
License and terms: see end of document.

Abstract

The development of peptide stapling techniques to stabilise α-helical secondary structure motifs of peptides led to the design of modulators of protein–protein interactions, which had been considered undruggable for a long time. We disclose a novel approach towards peptide stapling utilising macrocyclisation by late-stage Suzuki–Miyaura cross-coupling of bromotryptophan-containing peptides of the catenin-binding domain of axin. Optimisation of the linker length in order to find a compromise between both sufficient linker rigidity and flexibility resulted in a peptide with an increased α-helicity and enhanced binding affinity to its native binding partner β-catenin. An increased proteolytic stability against proteinase K has been demonstrated.

Introduction

Peptide cyclisation emerged as a popular approach to limit conformational mobility in order to enhance the binding affinity towards a biological target. Moreover, cyclic peptides are more stable against proteolytic digestion and can provide an improved membrane permeability [1-3]. Hence, peptide-based drugs became of high interest because of their high selectivity combined with low toxicity. Cross-linking of side chain residues results in constrained conformations and can be used to stabilise α-helical secondary structures. This technique is called peptide stapling and the most prominent methodology was de-

veloped by the groups of Grubbs and Verdine using ring-closing metathesis (RCM) [4-6]. The optimised protocol for these so-called hydrocarbon-stapled peptides uses α-methyl-, α-alkenylglycines in a distance of i, $i + 3/i + 4$ for one helix turn or i, $i + 7$ for two helix turns, respectively, followed by Ru-catalysed cross-linking [7]. By this robust and reliable approach, a library of stapled peptides was generated influencing diverse α-helical dominated protein–protein interactions (PPI) spanning pathways involved in cancer, infectious diseases, metabolic diseases and neurological disorders [8], which had been considered undruggable for a long time due to their large contact area and shallow surface [9]. Since then, many other reactions have been investigated for macrocyclisation with the objective of peptide stapling [10] including lactam- [11,12], disulfide- [13], thioether- [14-20], triazole- [21,22], oxime- [23] and hydrazone formation [24] as well as multicomponent reactions such as the Ugi- or Petasis reaction [25-32]. The content of helicity can moreover be changed by the introduction of a photo-switchable azobenzene staple [33,34]. Moreover, it has been shown that Pd-mediated cross-couplings can be successfully employed in the generation of cyclic and conformationally stabilised peptides. The groups of Buchwald, Pentelute, and Ackermann pioneered the development of Pd-mediated arylation chemistry of biomolecules [35-37]. The approaches by Buchwald and Pentelute are suitable for selective, bioorthogonal labelling of cysteine- [38-40] and lysine-containing [41,42] peptides and proteins using stochiometric amounts of preformed Pd(II)-aryl complexes. They can further be applied for peptide macrocyclisation of the two above mentioned side chain residues of the natural amino acids. However, these Pd-mediated stapling reactions were performed only on an analytical scale and the secondary structures of the cyclic peptides were not studied. Since tryptophan has only an incidence of about 1% in proteins, but is highly conserved in binding sites on protein surfaces mediating PPI [43], it is an attractive target for the development of selective diversifications. C–H activation of the indole C^2 position by Pd-catalysis allows both selective arylation [44-48] and formation of macrocycles [49]. The macrocyclisation technique by tryptophan C^2–H activation has been further improved showing structurally constrained peptides bearing a side chain connection of tryptophan and phenylalanine or tyrosine [50]. Moreover, a similar Pd-mediated approach for $C(sp^3)$–H activation of phthaloyl-protected *N*-terminal alanine was also used for macrocyclisation in peptide stapling [51,52].

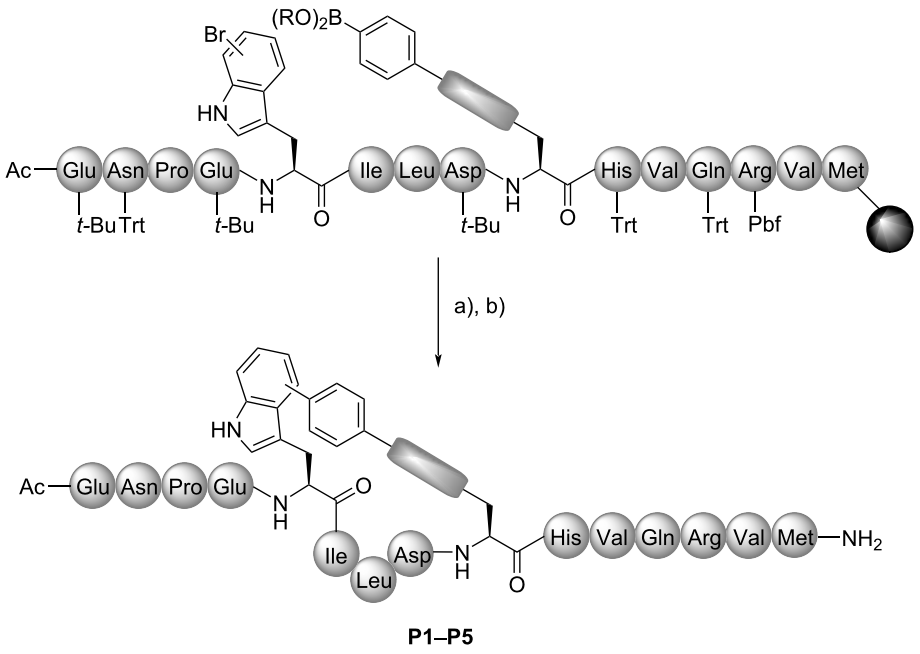
Besides addressing the indole C^2, the regioselective enzymatic halogenation at C5, C6, or C7 using FAD-dependent tryptophan halogenases opens a broad area of Pd-catalysed late-stage diversifications [53-55]. It has been proven that Pd-catalysed cross-couplings are very versatile tools for selective and bio-orthogonal modifications of haloindoles, halotryptophans and halotryptophan-containing peptides as well as natural products [56-70]. Additionally, halotryptophans were incorporated in pentapeptides as building blocks for macrocyclisation by Suzuki–Miyaura cross-coupling (SMC) aiming at the preparation of bicyclic peptides [71]. Recently, intramolecular SMC has been successfully applied to side chain-to-tail cyclisation between halotryptophans and boronic acids resulting in RGD peptides with high affinity towards integrin $\alpha_V\beta_3$, good selectivity and high plasma stability [72].

Results and Discussion

Design and synthesis of SMC stapled peptides

The intramolecular SMC was envisaged as a novel approach towards one-component peptide stapling by side chain cross-linking of bromotryptophan and an organoboron moiety. Bromotryptophans are accessible by enzymatic bromination utilising cross-linked enzyme aggregates (combiCLEAs) containing an FAD-dependent tryptophan halogenase, a flavin reductase and an alcohol dehydrogenase [73,74]. For this purpose, tryptophan halogenases RebH and Thal were applied for the generation of L-7-bromo- and L-6-bromotryptophan, respectively. As a peptide sequence, we chose the β-catenin-binding domain (CBD) of axin as a benchmark system (PDB ID 1QZ7) [75]. Axin is a scaffold protein playing an essential part in the destruction complex for β-catenin labelling in the canonical Wnt signalling. Loss-of-function mutations in this pathway lead to a dysregulated signal transduction causing cancer [75,76]. All-hydrocarbon stapled peptides comprising amino acids 467 to 481 of the axin CBD had been studied in the group of Verdine and evaluation of optimised staple positions at amino acids 471 (i) and 475 ($i + 4$) resulted in enhanced helicity and binding affinity to β-catenin, e.g., for peptide **StAx-3** [77]. Following the **StAx-3** peptide, we designed peptides including bromotryptophan in *i*-position and an organoboron containing side chain in the $i + 4$-position. The peptides were synthesised on Rink amide resin by solid-phase peptide synthesis (SPPS) with Fmoc/*t*-Bu strategy followed by on-resin SMC. For the cross-coupling, a modified protocol by Planas and co-workers was used [78]. $Pd_2(dba)_3$ was employed as the Pd source together with the water-soluble Buchwald ligand sulfonated SPhos (sSPhos) and potassium fluoride as a base. The reaction was performed in a solvent mixture of dimethoxyethane, ethanol and water (DME/EtOH/H_2O 9:9:2) at 120 °C under microwave irradiation for 30 min (Scheme 1) [78].

The studies were initiated with a macrocyclisation between a 7-bromotryptophan and a 4-pinacolatoborono phenylalanine

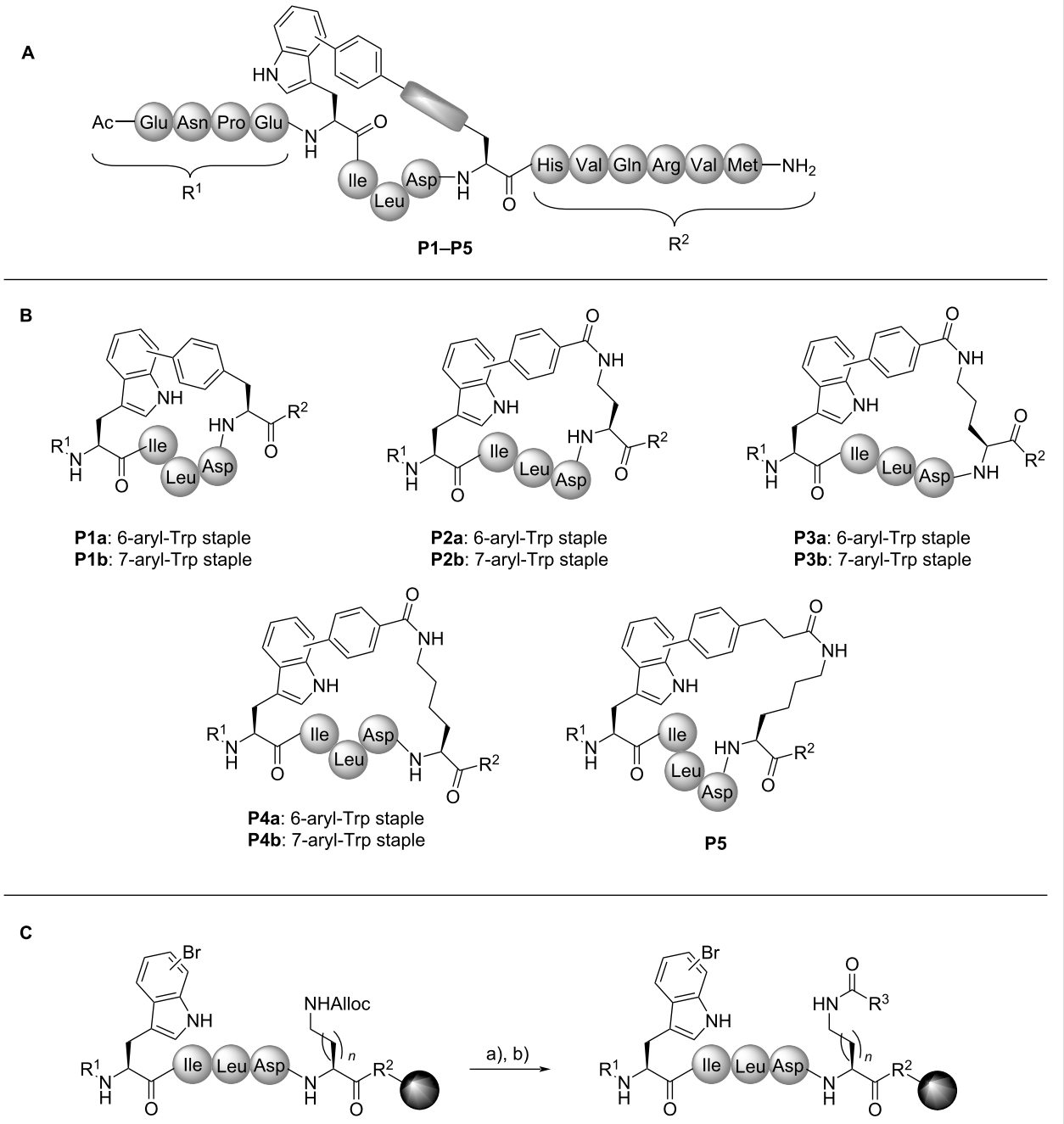


Scheme 1: Synthesis of SMC stapled axin CBD peptides. Reaction conditions: (a) $Pd_2(dba)_3$, sSPhos, KF, DME/EtOH/H_2O 9:9:2, 120 °C, μwave, 30 min; (b) TFA/TIS/H_2O 95:2.5:2.5, DTT, phenol, 2 × 2 h. $B(OR)_2$ = $B(OH)_2$, B(pin), pin = pinacolato, *t*-Bu = *tert*-butyl, Trt = trityl, Pbf = pentamethyldihydrobenzofuran-5-sulfonyl.

side chain to generate the cyclic peptide **P1b** (Scheme 2A and B). The intramolecular SMC took place with full consumption of the starting material and without formation of an intermolecular macrocyclisation product, which was confirmed by MALDI-ToF-MS of the crude reaction mixture after test cleavage (see Supporting Information File 1, Figure S1). However, deboronation and dehalogenation were observed as side reactions to some extent as well as oxidation, most likely of methionine (Met) [79]. The oxidation could be minimised by improved cleavage conditions under argon. Replacing sSPhos by tri(*o*-tolyl)phosphine (P(*o*-Tol)$_3$), that had successfully been applied for peptide cyclisation by on-resin SMC [78,80], led to incomplete conversion.

The cyclisation of the same peptide with the regioisomer 6- instead of 7-bromotryptophan yielded the expected stapled peptide **P1a**. Next, the secondary structures of the two stapled peptides **P1a** and **P1b** were investigated by CD spectroscopy. Unfortunately, both peptides did not show enhanced helical conformation in water. To get more information about the structure, the spectra were also recorded in a mixture of 2,2,2-trifluoroethanol (TFE)/water 4:1 since TFE promotes the formation of helices [81]. Interestingly, the helical structure could be slightly enhanced but this effect was not as pronounced as for the linear parent peptide aAxWt in TFE/water 4:1 (see Supporting Information File 1, Figure S4).

As a conclusion from those experiments, it was hypothesised that the linker might be too rigid resulting in a distorted structure, which has also been previously reported for thioether cross-linked cysteines bearing a biphenyl template within the staple [20]. Hence, a linker with a higher degree of flexibility was designed. This goal was achieved by a modification of amine-containing amino acids in the $i + 4$ position through coupling to 4-carboxyphenylboronic acid, followed by intramolecular SMC. Different linker lengths were achieved by introducing L-2,4-diaminobutyric acid (Dab), ornithine (Orn), or lysine (Lys). Utilising the Alloc protecting group allowed the coupling of 4-carboxyphenylboronic acid once the linear sequence had been synthesised (Scheme 2C). The intramolecular SMC between 6- or 7-bromotryptophan and the boronic acid afforded the stapled peptides **P2** to **P4** with complete conversion (Scheme 2B). LC–MS analyses revealed broadened or two signals for peptides **P1** to **P4**, which were inseparable by preparative RP-HPLC purification (see Supporting Information File 1). The presence of more than one isomer may be due to the co-existence of diastereomers, i.e. *cis*/*trans* isomers or conformers with a high interconversion barrier. For complestatin-based macrocyclic peptides, the existence of biaryl atropisomers caused by the indole of tryptophan has been reported [82]. Recently, the occurrence of isomers was also observed in our group for SMC cyclised RGD peptides. It could be proven that an isomerisation is not caused by the cross-



Scheme 2: Overview of the different cross-linkages obtained by intramolecular SMC. A) General structure of SMC stapled axin CBD peptides. B) Overview of different cross-links: For peptides **P1** to **P4**, 6- and 7-aryl-Trp staples were synthesised, peptide **P5** was only generated with 7-aryl-Trp staple. C) On-resin modification of amines (n = 1: Dab, n = 2: Orn, n = 3: Lys) in i + 4 position to obtain organoboron side chains with increased linker flexibility. Reaction conditions: (a) $Pd(PPh_3)_4$, morpholine in DCM, 2 × 20 min; (b) carboxylic acid, HATU, DIEA in DMF, 1 h. In panel C), amino acids in R^1 and R^2 are with protecting groups and R^2 is resin-bound (Rink amide resin); R^3 = 4-phenylboronic acid or (4-ethylphenyl)boronic acid (**P2–P5**).

coupling but by the presence of stable isomers/conformers. Molecular dynamics (MD) simulations verified the appearance of stable, distinct conformers or atropisomers, which were in accordance with the experimental data [72]. Moreover, the epimerization by the conditions of SMC is unlikely as it has been excluded by total hydrolysis of a late-stage SMC modified RGD peptide [67].

Analysis of the secondary structures of the cyclic peptides **P2–P4** by CD spectroscopy also did not show a significantly increased α-helicity in water. Investigation of several derivatives by means of density functional theory (DFT) geometry optimisations indicated that substitution at indole C^6 tends to induce more significant deformation of the peptide chain compared to substitution at indole C^7. Moreover, introduction of an addition-

al ethylene unit in the linker suggested a conformation with the highest similarity to the linear reference peptide **P6** (see Supporting Information File 1), thus representing a good compromise between rigidity and preservation of the target secondary structure. Serine in *i*-position and glutamic acid in *i* + 4-position of the linear axin CBD sequence ***a*AxWt** were substituted by tryptophan and lysine, respectively, to have a higher analogy to the lysine modified SMC stapled peptides. Following the indications of DFT calculations, stapled peptide **P5** was synthesised by modification of lysine in the *i* + 4-position with 4-(2-carboxyethyl)phenylboronic acid followed by on-resin SMC (Scheme 2B).

LC–MS analysis revealed two isobaric peaks indicating two isomers, which were largely separable by preparative HPLC with the less polar isomer **P5.2** being the major one. The secondary structures of both isomers were investigated by CD spectroscopy and an increased helicity was observed for both peptides. In particular, **P5.2** shows the characteristic signature of an α-helix with the tendency of minima at λ = 208 and 222 nm and a maximum at λ = 190 nm (Figure 1). The CD spectra provided calculated helicities of 9% for ***a*AxWt**, 15% for **P5.1**, and 21% for **P5.2** (see Supporting Information File 1).

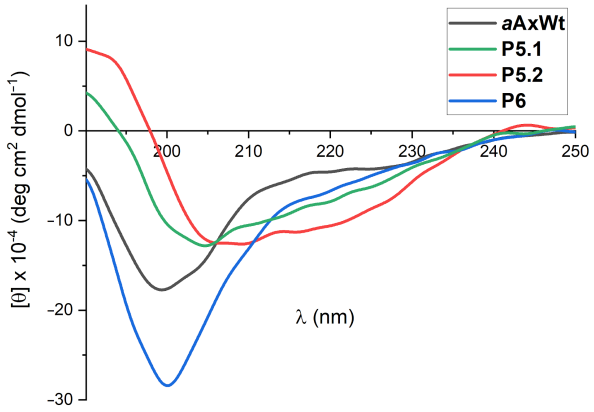


Figure 1: Analysis of the secondary structure by circular dichroism: CD spectra of both isomers of stapled peptide **P5** (**P5.1** and **P5.2**) and linear references (***a*AxWt**, **P6**) (*c* = 100 μM) at 20 °C in water.

Biological evaluation

Competitive fluorescence polarisation (FP) assays were performed to evaluate whether the increased helicity of peptide **P5** also results in an increased binding affinity to its native binding partner β-catenin. The *N*-terminal FITC-labelled RCM-stapled peptide ***f*StAx-3** was synthesised as tracer for this study and its dissociation constant was determined to be 63 ± 6 nM in a direct fluorescence polarisation assay, which is in agreement with previously reported data [77]. Noteworthy, the isomer **P5.2** of stapled peptide **P5** shows an almost five times higher binding affinity (K_d = 258 ± 43 nM) compared to the linear reference peptide **P6** (K_d = 1241 ± 162 nM, Figure 2) in the competitive FP assay. Isomer **P5.1** was only isolated in insufficient amounts. Hence, a satisfactorily converging inhibition curve could not be obtained since it requires high inhibitor concentrations. In addition, the wild-type sequence ***a*AxWt** was also tested in the competitive FP assay (K_d = 1448 ± 204 nM) against its FITC-labelled analogue ***f*AxWt**, which had been determined in a direct assay (K_d = 1191 ± 182 nM).

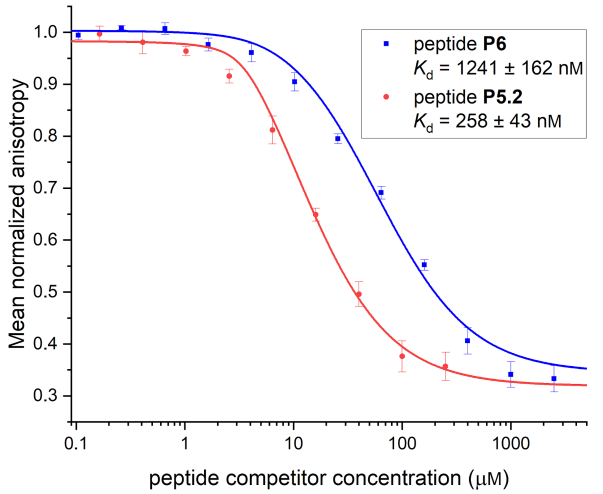


Figure 2: In vitro binding affinities to β-catenin determined by competitive fluorescence polarisation assays.

Finally, the stability of both peptides **P5** and **P6** was tested against proteinase K digestion. Whilst the linear analogue **P6** is cleaved within a period of 120 min to give three fragments, the stapled peptide **P5** allows access to only one of the three cleavage sites: i.e., proteolysis of the Leu–Asp bond within the macrocycle and of the Lys–His bond, which is part of the cross-link, is prevented by the stapling (Figure 3 and Supporting Information File 1, Figures S8 to S10).

Conformational analysis

The identification of two isomers of **P5** by LC–MS led us investigate the possibility of diastereomers and conformers in the macrocycle. The amide bond in the staple of **P5** is connected to two flexible aliphatic chains and may exist in *cis* and *trans* configuration. The energy difference in the analogue *N*-methylacetamide (NMA) favours the *trans* isomer by about 2.3 kcal mol^{-1}, which corresponds to an expected *cis*/*trans* ratio of about 1:44 at 300 K, with an interconversion barrier of 18.7 kcal mol^{-1} [83]. The experimental **P5.1**/**P5.2** ratio is nearly 1:3, suggesting an energy difference of only 0.9 kcal mol^{-1} in favour of **P5.2**. Strain in the macrocycle might be responsible for such slight decrease in the relative energy between the *cis*

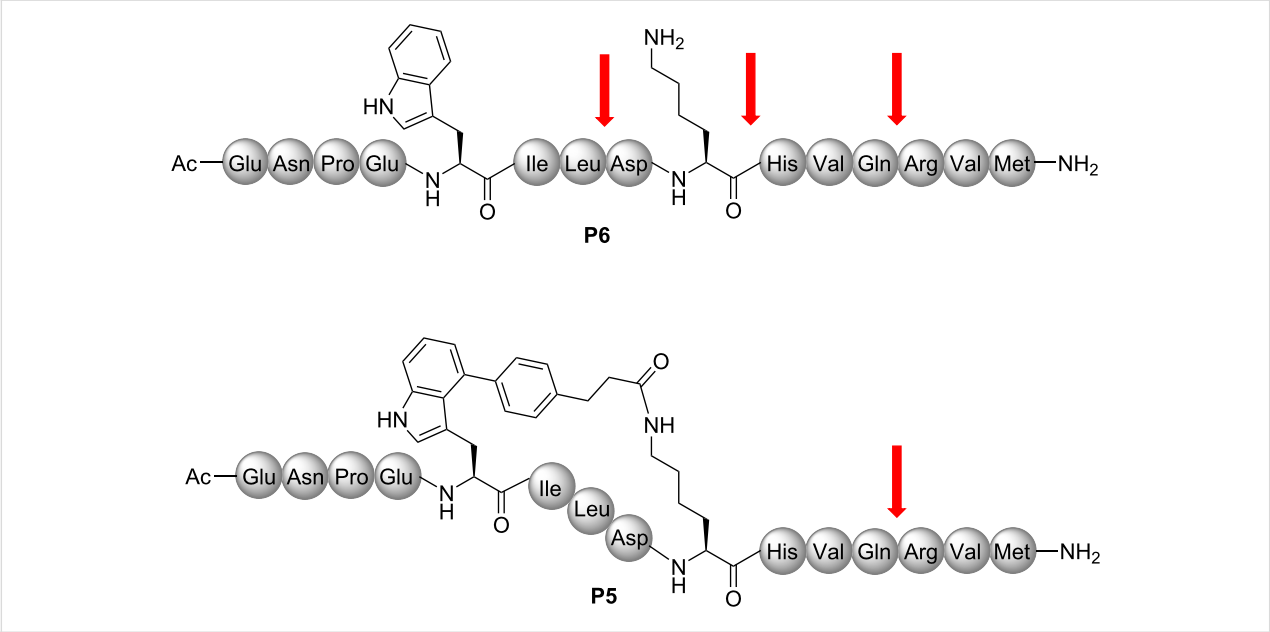


Figure 3: Cleavage sites of Proteinase K digestion indicated by a red arrow.

and *trans* isomers compared to isolated NMA. The presence of diastereomers in the peptide bonds is less likely since the *cis*/*trans* ratio in polypeptides is lower than 1:820 (i.e., an energy difference greater than 4.0 kcal mol^{-1} in favour of the *trans* isomer) [84]. It is, however, currently hopeless to expect catching energy differences as small as that between **P5.1**/**P5.2** by molecular modelling. Instead, we discuss qualitatively the conformational properties of the macrocycle in the two diastereomers of **P5** to determine if conformers may exist with high interconversion barriers, and suggest an assignment based on other experimental observables, namely, the flexibility of the overall peptide and its propensity to form a helical secondary structure. We then proceed to analyse the effect of the staple and sequence variations on the secondary structure of the peptidic backbone of ***a*AxWt**, **P5**, and **P6**.

The conformational preferences of the stapled peptide **P5** and of the linear peptides **P6** and ***a*AxWt** were investigated via extensive accelerated molecular dynamics simulations (aMD) as implemented within the Amber18 program package [85]. The aMD methodology developed by McCammon and co-workers [86] has shown to be a highly effective tool to sample the conformational space of polypeptides made of sequences of 10 to 30 amino acids [87,88] and of macrocycles [89]. Our simulation strategy, mainly adapted from the latter references, made use of 15 independent 700 ns-long aMD simulation runs for each peptide (i.e., a cumulative total of 10.5 μs per peptide) performed with the ff14SB/GAFF [90,91] and TIP4Pew [91] force field parameters for the peptides and water, respectively, as well as specifically derived parameters for non-standard residues of the linker in stapled peptide **P5**. The conformation of the macrocycles was analysed via principal component analysis (PCA) of the non-hydrogen atoms forming the cycle, and the structure of the peptide backbone was investigated via secondary structure analysis and backbone root mean square deviation (RMSD) clustering including amino acids Pro^3 to Met^{15}. Time-averaged analysis was performed on the ensemble of structures obtained from the last 500 ns of each simulation run (i.e., a cumulative total of 7.5 μs per peptide; see Supporting Information File 1 for further methodological details and extended analysis).

Figure 4 summarises the conformational analysis on the macrocycle in the *cis* and *trans* isomer form of **P5**. PCA reveals that the first three principal components (PCs) respectively capture 39.0, 21.3, and 13.4% of the total variance in **P5** *cis*, and 31.2, 25.4, and 9.9% in **P5** *trans*. PCA-based clustering with a minimum distance of 4.0 Å in the three-dimensional space of PC1-3 led to 32 and 38 structural clusters for the *cis* and *trans* isomers, respectively. The first three representative structures are depicted in Figure 4, the first six clusters are projected in the three-dimensional space of PC1-3, and the corresponding representative structures are indicated in the two-dimensional projection in the space of PC1 and PC2, where colouring is made by relative free energy as obtained from Boltzmann reweighting using 10^{th} order Maclaurin series expansion [92,93]. In both isomers, the first three clusters represent about 53% of the total conformational space of the macrocycle. *Cis* and *trans* isomers share a fairly similar main conformation (c1, blue in the figure) with high population (31.8 and 27.9%, respectively). This con-

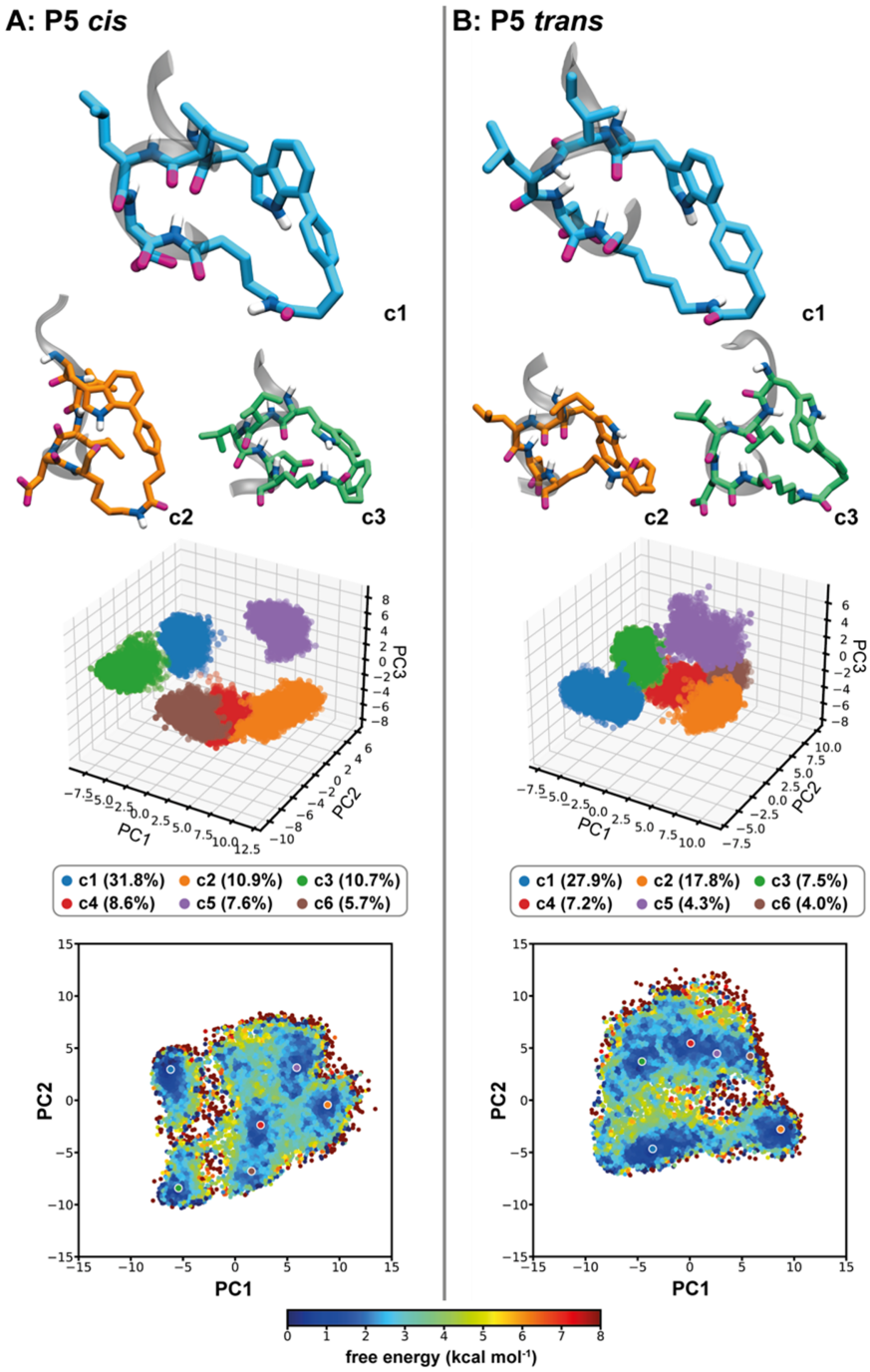


Figure 4: Principal component analysis (PCA) of the macrocycle's non-hydrogen atoms in the two isomers of **P5**. The upper panel depicts the three main conformations of the macrocycle in **P5** *cis* (column A) and **P5** *trans* (column B) shown in liquorice. Aliphatic hydrogen atoms are hidden and a ribbon representation of the peptidic backbone is shown in grey. Other amino acids in the sequence are not shown in the figure although present in the simulations. The middle panel shows the three-dimensional projection of the six main PCA-based conformational clusters in the space of the first three principal components (PC). The lower panel presents a two-dimensional projection in the plane of the first two PCs. Each point corresponds to a trajectory frame and is coloured according to its corresponding re-weighted relative free energy. Data is calculated on the cumulative last 500 ns of 15 accelerated molecular dynamics runs for each SMC peptide.

formation is stabilised by a hydrogen bond between the CO group of Ile and the NH group of Lys, and triggers the formation of a helical structure in the peptidic portion of the macrocycle. Conformation c2 of the *cis* isomer (10.9%) presents the Leu side chain pointing towards the centre of the macrocycle and leads to a disruption of helicity. The third conformation for

this isomer (c3 with 10.7%) is also helical in the peptidic portion of the macrocycle and is similar to c1, with the Trp's indole group pointing in the other direction. In the *trans* isomer, both conformations are also found, however, with different populations and order. Conformation c2 of **P5** *trans* is helical and resembles c3 of **P5** *cis*, yet with a significantly higher probability of occurrence (17.8%). The non-helical conformation c3 of **P5** *trans* (7.5%) is slightly less populated than the corresponding c2 of **P5** *cis*. The macrocycle of both isomers is found to be rather flexible, forming well-separated conformational clusters in the three-dimensional space of PC1-3. The projection in the two-dimensional space of PC1 and PC2 indicates that the conformers are interconnected with barriers lower than 6 kcal mol^{-1}. It is worth noting, that the barriers are likely to be overestimated due to a poor sampling of transition structures compared to local minima. More accurate values would be obtained with methods better adapted for kinetics, such as Markov models (for a general overview see reference [94]). Yet, such low barriers are not sufficient to trap the SMC peptide in conformations that can be separated experimentally at ambient conditions [95] and the analysis therefore rules out the possibility of conformational isomers, within the limits of exhaustivity of our sampling. The *cis*/*trans* conversion barrier is likely to be close to that of isolated NMA, and leads us to conclude that the two isomers isolated experimentally are diastereomers of the amide bond in the staple of **P5**.

The secondary structure analysis of the three peptides ***a*AxWt**, **P5** (*cis* and *trans*) and **P6** is summarized in Figure 5. Figure 5A reports the percentage of amino acids adopting a given secondary structure over the simulation time. All peptides show a significant fraction of amino acids in an α-helical conformation, with a smaller yet substantial propensity to participate in turns and bends. Overall, **P5** *trans* is the most helical peptide, followed by ***a*AxWt**, and **P5** *cis*, and **P6** is significantly less helical than the others, in terms of individual amino acid's contributions. **P6** stands out with a fairly high fraction of amino acids present in an anti-parallel β-sheet backbone conformation. ***a*AxWt** also shows a small fraction of anti-parallel β-sheet, while **P5** *trans* only shows a marginal percentage of parallel β-structure. The backbone RMSD-based clustering further breaks down the conformational preferences of the three peptides and is summarized in Figure 5B–E showing the representative structures of the first four structural clusters. The main conformation of ***a*AxWt**, **P5** *cis*, and **P5** *trans* is highly populated (23.3, 19.4, and 19.7%, respectively), and shows a full α-helix that closely resembles the active conformation of axin's binding domain (superimposed in transparent grey). **P6** also forms a similar α-helix with a fairly high probability (14.7%). However, the main conformation of **P6** (26.2%) is found to be formed by two β-sheets linked by a turn at the middle of the sequence. The second and third conformations of ***a*AxWt**, **P5** *cis*, and **P5** *trans* are also significantly helical, with helices formed by at least six consecutive amino acids. The fourth conformation of ***a*AxWt** is a β-structure resembling the main geometry of **P6**. Overall, ***a*AxWt**, **P5** *cis*, and **P5** *trans* form helices made of at least six consecutive amino acids with a cumulative probability of 33.1, 37.5, and 45.2%, respectively. Noteworthy, these percentages are not re-weighted and are, therefore, somewhat biased by the aMD protocol. Yet, trends should be qualitatively captured by the analysis, which correlates fairly well with the experimental results in Table S1 (Supporting Information File 1).

The mutations from ***a*AxWt** to **P6** result in a significant change in conformational preferences and the probability of stable β-structures in the latter. This observation is consistent with the CD spectrum of **P6** that presents β-sheets features. The staple in **P5** successfully quenches such biologically unfavourable conformation and significantly increases the probability of forming helical structures that closely resemble the active conformation of axin's binding domain. Both, *cis* and *trans* isomers form α-helices with a high probability, yet the *trans* isomer tends to be more helical than the *cis* variant. The CD spectra of **P5.1** and **P5.2** indicate that the latter has a more helical character, which leads us to speculate that **P5.1** corresponds to the *cis* diastereomer, while **P5.2** presents the amide bond in the staple in a *trans* configuration. Furthermore, analysis of the structural diversity of the two isomers of **P5** indicates that **P5** *cis* (**P5.1**) is more disordered (see Supporting Information File 1, Table S3), which also correlates with a blue-shifted absorption minimum compared to **P5** *trans* (**P5.2**).

In the partially helical structures of ***a*AxWt** (i.e., second and third conformations in Figure 5b), the helix is formed in the second half of the sequence. In **P5** *cis* and **P5** *trans*, however, the second conformation presents the beginning of the sequence with a helical structure, including the amino acids that participate in the macrocycle. While possible, it would be speculative to link this property of the **P5** to its enhanced biological activity. Instead, we find a more likely reason for the greater activity of **P5.2** over that of ***a*AxWt** in analysing the conformational diversity of the two peptides (see Supporting Information File 1, Table S2). In **P5** *trans* (identified as **P5.2**), 60% of the conformational space is represented by the first 7 structural clusters against 18 for ***a*AxWt**. The latter is, therefore, significantly more flexible and may be found more often in a non-active conformation, including β-structures, compared to **P5.2**. This last observation tends to correlate with a higher binding affinity of **P5.2** over its linear counterparts. Although all peptides can form an α-helix that resembles the active form of axin's binding domain, **P6** and ***a*AxWt** occur often in other con-

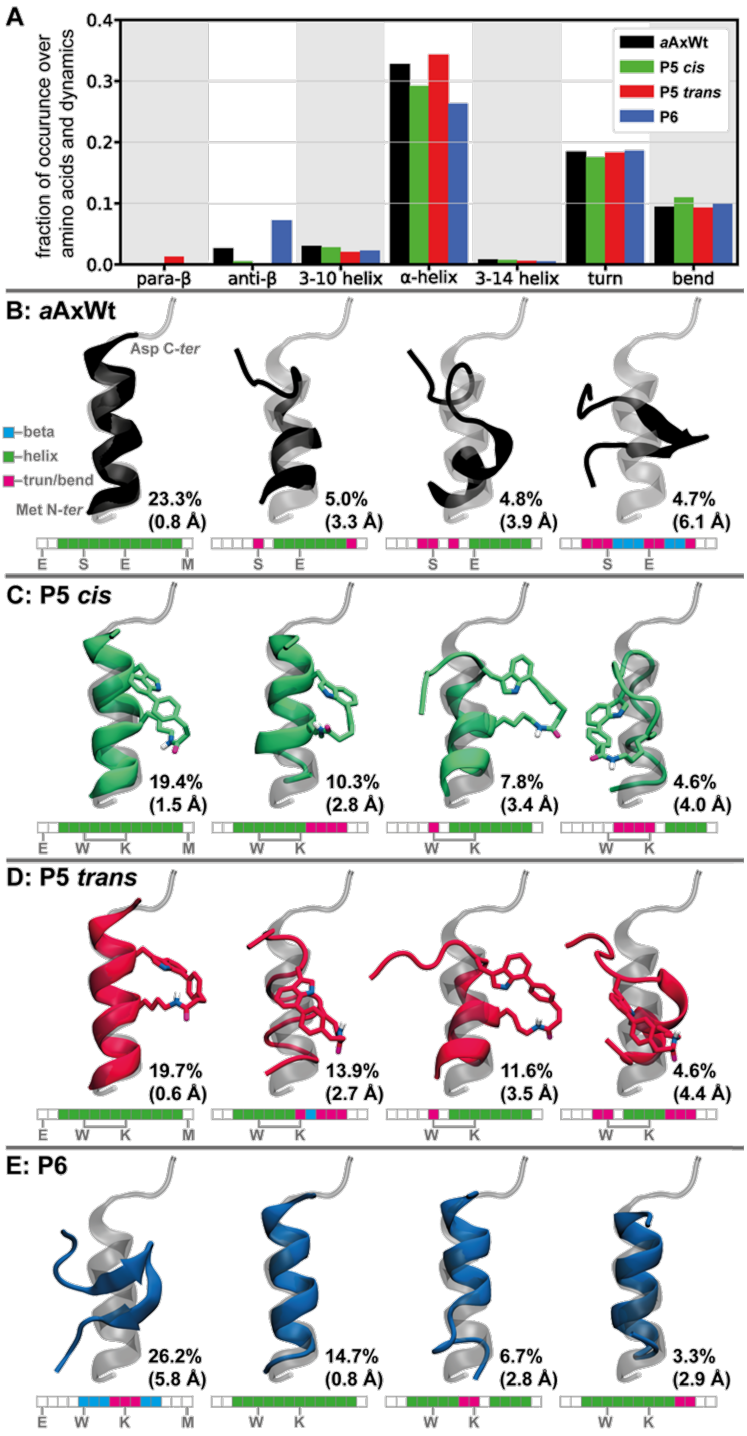


Figure 5: Molecular modelling of the conformational preferences of the SMC stapled peptides **P5** (with *cis* or *trans* amide bond in the staple), and the linear references **P6** and ***a*AxWt** by means of accelerated molecular dynamics (aMD). A. Secondary structure analysis showing the fraction of amino acids found in a specific backbone conformation as normalised over the full sequence and the cumulative last 500 ns of 15 aMD runs for each peptide. B. Results of structural clustering analysis for peptide ***a*AxWt**. The representative structure (black) of the four main structural clusters are depicted superimposed to the active conformation of axin's binding domain (in transparent grey; PDB ID 1QZ7) [75]. Cluster populations are given next to the respective structure and backbone-atoms root mean square deviation with respect to the active conformation are indicated in parenthesis. RMSD reported and used in clustering were calculated from Pro to Met only. A schematic representation of the secondary structure of each amino acid is given bellow the representative structures as obtained from an average over the whole cluster (beta structures in blue, helices in green, and turn/bend in pink). C–E. Same as panel B for **P5.1** (green), **P5.2** (red), and **P6** (blue), respectively. **P5.1** and **P5.2** differ in the conformation of the amide bond in the staple (*cis* and *trans*, respectively).

formations that are rather far from the active one. Overall, when presenting the peptides to the target domain of β-catenin, **P6** and ***a*AxWt** are substantially less likely to be in an active or near-active conformation compared to **P5.2**. In the ensemble of conformations, the fraction of active ones is therefore greater for **P5.2**, which translates into a greater binding affinity measured experimentally.

Conclusion

In conclusion, suitable reaction conditions were found for the synthesis of stapled peptides by an intramolecular late-stage SMC on resin. The peptide sequences are based on the CBD of axin. Optimisation of the cross-link, guided by DFT geometry optimisation, finally resulted in SMC stapled peptide **P5** showing an increased α-helicity. Compared to the linear analogue **P6**, **P5** revealed a five times higher binding affinity to its native binding partner β-catenin. A proteinase K stability assay demonstrated higher stability of the stapled peptide **P5** against proteolytic digestion because two of the three cleavage sites are blocked by the macrocycle. Accelerated molecular dynamics simulations verified a significantly higher degree of helicity for SMC stapled peptide **P5** compared to the linear analogues **P6** and ***a*AxWt**, which is in accordance with the experimental data obtained from CD and moreover, explains the increased binding affinity to β-catenin as **P5** is more likely to be found in an active conformation.

Supporting Information

Supporting Information File 1

Details on the amino acid and peptide synthesis, analytical data of the peptides, CD spectroscopy, β-catenin expression and purification, fluorescence polarization assay, proteinase K stability assay, and theoretical methods.
[https://www.beilstein-journals.org/bjoc/content/supplementary/1860-5397-18-1-S1.pdf]

Acknowledgements

The authors thank A. Nieß, M. Wißbrock, and P. Borchert for technical assistance. A. Merschel and K. D. Stuke are acknowledged for support in the synthetic work.

Funding

The project was supported in part by a Bielefeld University Ph.D. fellowship to H.G. and by Deutsche Forschungsgemeinschaft (SE609/16-1). The DFT calculations were carried out using hardware and software resources of the Supercomputing and Networking Center in Wroclaw (grant no. 197). R.M. and A.M. gratefully acknowledge the support of NVIDIA Corporation with the donation of a Titan Xp GPU used for this research as well as TUBITAK ULAKBIM High Performance and Grid Computing Center (TRUBA resources) for additional calculations.

ORCID® iDs

Hendrik Gruß - https://orcid.org/0000-0001-7267-9663
Rebecca C. Feiner - https://orcid.org/0000-0002-8784-0875
Ridhiwan Mseya - https://orcid.org/0000-0001-7622-6370
Michał Jewgiński - https://orcid.org/0000-0003-4931-5452
Kristian M. Müller - https://orcid.org/0000-0002-7914-0625
Antoine Marion - https://orcid.org/0000-0002-8266-8957
Norbert Sewald - https://orcid.org/0000-0002-0309-2655

References

1. Valeur, E.; Guéret, S. M.; Adihou, H.; Gopalakrishnan, R.; Lemurell, M.; Waldmann, H.; Grossmann, T. N.; Plowright, A. T. *Angew. Chem., Int. Ed.* **2017,** *56,* 10294–10323. doi:10.1002/anie.201611914
2. Valeur, E.; Guéret, S. M.; Adihou, H.; Gopalakrishnan, R.; Lemurell, M.; Waldmann, H.; Grossmann, T. N.; Plowright, A. T. *Angew. Chem.* **2017,** *129,* 10428–10459. doi:10.1002/ange.201611914
3. Verdine, G. L.; Hilinski, G. J. *Drug Discovery Today: Technol.* **2012,** *9,* e41–e47. doi:10.1016/j.ddtec.2012.01.004
4. Blackwell, H. E.; Grubbs, R. H. *Angew. Chem., Int. Ed.* **1998,** *37,* 3281–3284. doi:10.1002/(sici)1521-3773(19981217)37:23<3281::aid-anie3281>3.0.co;2-v
5. Blackwell, H. E.; Grubbs, R. H. *Angew. Chem.* **1998,** *110,* 3469–3472. doi:10.1002/(sici)1521-3757(19981204)110:23<3469::aid-ange3469>3.0.co;2-a
6. Schafmeister, C. E.; Po, J.; Verdine, G. L. *J. Am. Chem. Soc.* **2000,** *122,* 5891–5892. doi:10.1021/ja000563a
7. Kim, Y.-W.; Grossmann, T. N.; Verdine, G. L. *Nat. Protoc.* **2011,** *6,* 761–771. doi:10.1038/nprot.2011.324
8. Walensky, L. D.; Bird, G. H. *J. Med. Chem.* **2014,** *57,* 6275–6288. doi:10.1021/jm4011675
9. Dömling, A. *Protein-protein interactions in drug discovery;* Wiley-VCH: Weinheim, Germany, 2013.
10. Lau, Y. H.; de Andrade, P.; Wu, Y.; Spring, D. R. *Chem. Soc. Rev.* **2015,** *44,* 91–102. doi:10.1039/c4cs00246f
11. Felix, A. M.; Heimer, E. P.; Wang, C. T.; Lambros, T. J.; Fournier, A.; Mowles, T. F.; Maines, S.; Campbell, R. M.; Wegrzynski, B. B.; Toome, V.; Fry, D.; Madison, V. S. *Int. J. Pept. Protein Res.* **1988,** *32,* 441–454. doi:10.1111/j.1399-3011.1988.tb01375.x
12. Shepherd, N. E.; Hoang, H. N.; Abbenante, G.; Fairlie, D. P. *J. Am. Chem. Soc.* **2005,** *127,* 2974–2983. doi:10.1021/ja0456003
13. Jackson, D. Y.; King, D. S.; Chmielewski, J.; Singh, S.; Schultz, P. G. *J. Am. Chem. Soc.* **1991,** *113,* 9391–9392. doi:10.1021/ja00024a067
14. Brunel, F. M.; Dawson, P. E. *Chem. Commun.* **2005,** 2552–2554. doi:10.1039/b419015g
15. Brunel, F. M.; Zwick, M. B.; Cardoso, R. M. F.; Nelson, J. D.; Wilson, I. A.; Burton, D. R.; Dawson, P. E. *J. Virol.* **2006,** *80,* 1680–1687. doi:10.1128/jvi.80.4.1680-1687.2006
16. Wang, Y.; Chou, D. H.-C. *Angew. Chem., Int. Ed.* **2015,** *54,* 10931–10934. doi:10.1002/anie.201503975

17. Wang, Y.; Chou, D. H.-C. *Angew. Chem.* **2015,** *127,* 11081–11084. doi:10.1002/ange.201503975
18. Zhang, G.; Barragan, F.; Wilson, K.; Levy, N.; Herskovits, A.; Sapozhnikov, M.; Rodríguez, Y.; Kelmendi, L.; Alkasimi, H.; Korsmo, H.; Chowdhury, M.; Gerona-Navarro, G. *Angew. Chem., Int. Ed.* **2018,** *57,* 17073–17078. doi:10.1002/anie.201810007
19. Zhang, G.; Barragan, F.; Wilson, K.; Levy, N.; Herskovits, A.; Sapozhnikov, M.; Rodríguez, Y.; Kelmendi, L.; Alkasimi, H.; Korsmo, H.; Chowdhury, M.; Gerona-Navarro, G. *Angew. Chem.* **2018,** *130,* 17319–17324. doi:10.1002/ange.201810007
20. Jo, H.; Meinhardt, N.; Wu, Y.; Kulkarni, S.; Hu, X.; Low, K. E.; Davies, P. L.; DeGrado, W. F.; Greenbaum, D. C. *J. Am. Chem. Soc.* **2012,** *134,* 17704–17713. doi:10.1021/ja307599z
21. Scrima, M.; Le Chevalier-Isaad, A.; Rovero, P.; Papini, A. M.; Chorev, M.; D'Ursi, A. M. *Eur. J. Org. Chem.* **2010,** 446–457. doi:10.1002/ejoc.200901157
22. Kawamoto, S. A.; Coleska, A.; Ran, X.; Yi, H.; Yang, C.-Y.; Wang, S. *J. Med. Chem.* **2012,** *55,* 1137–1146. doi:10.1021/jm201125d
23. Haney, C. M.; Loch, M. T.; Horne, W. S. *Chem. Commun.* **2011,** *47,* 10915–10917. doi:10.1039/c1cc12010g
24. Madden, M. M.; Muppidi, A.; Li, Z.; Li, X.; Chen, J.; Lin, Q. *Bioorg. Med. Chem. Lett.* **2011,** *21,* 1472–1475. doi:10.1016/j.bmcl.2011.01.004
25. Vasco, A. V.; Méndez, Y.; Porzel, A.; Balbach, J.; Wessjohann, L. A.; Rivera, D. G. *Bioconjugate Chem.* **2019,** *30,* 253–259. doi:10.1021/acs.bioconjchem.8b00906
26. Ricardo, M. G.; Llanes, D.; Wessjohann, L. A.; Rivera, D. G. *Angew. Chem., Int. Ed.* **2019,** *58,* 2700–2704. doi:10.1002/anie.201812620
27. Ricardo, M. G.; Llanes, D.; Wessjohann, L. A.; Rivera, D. G. *Angew. Chem.* **2019,** *131,* 2726–2730. doi:10.1002/ange.201812620
28. Ricardo, M. G.; Ali, A. M.; Plewka, J.; Surmiak, E.; Labuzek, B.; Neochoritis, C. G.; Atmaj, J.; Skalniak, L.; Zhang, R.; Holak, T. A.; Groves, M.; Rivera, D. G.; Dömling, A. *Angew. Chem., Int. Ed.* **2020,** *59,* 5235–5241. doi:10.1002/anie.201916257
29. Ricardo, M. G.; Ali, A. M.; Plewka, J.; Surmiak, E.; Labuzek, B.; Neochoritis, C. G.; Atmaj, J.; Skalniak, L.; Zhang, R.; Holak, T. A.; Groves, M.; Rivera, D. G.; Dömling, A. *Angew. Chem.* **2020,** *132,* 5273–5279. doi:10.1002/ange.201916257
30. Reguera, L.; Rivera, D. G. *Chem. Rev.* **2019,** *119,* 9836–9860. doi:10.1021/acs.chemrev.8b00744
31. Ceballos, J.; Grinhagena, E.; Sangouard, G.; Heinis, C.; Waser, J. *Angew. Chem., Int. Ed.* **2021,** *60,* 9022–9031. doi:10.1002/anie.202014511
32. Ceballos, J.; Grinhagena, E.; Sangouard, G.; Heinis, C.; Waser, J. *Angew. Chem.* **2021,** *133,* 9104–9113. doi:10.1002/ange.202014511
33. Kumita, J. R.; Smart, O. S.; Woolley, G. A. *Proc. Natl. Acad. Sci. U. S. A.* **2000,** *97,* 3803–3808. doi:10.1073/pnas.97.8.3803
34. Flint, D. G.; Kumita, J. R.; Smart, O. S.; Woolley, G. A. *Chem. Biol.* **2002,** *9,* 391–397. doi:10.1016/s1074-5521(02)00109-6
35. Zhang, C.; Vinogradova, E. V.; Spokoyny, A. M.; Buchwald, S. L.; Pentelute, B. L. *Angew. Chem., Int. Ed.* **2019,** *58,* 4810–4839. doi:10.1002/anie.201806009
36. Zhang, C.; Vinogradova, E. V.; Spokoyny, A. M.; Buchwald, S. L.; Pentelute, B. L. *Angew. Chem.* **2019,** *131,* 4860–4892. doi:10.1002/ange.201806009
37. Wang, W.; Lorion, M. M.; Shah, J.; Kapdi, A. R.; Ackermann, L. *Angew. Chem., Int. Ed.* **2018,** *57,* 14700–14717. doi:10.1002/anie.201806250
38. Vinogradova, E. V.; Zhang, C.; Spokoyny, A. M.; Pentelute, B. L.; Buchwald, S. L. *Nature* **2015,** *526,* 687–691. doi:10.1038/nature15739
39. Rojas, A. J.; Pentelute, B. L.; Buchwald, S. L. *Org. Lett.* **2017,** *19,* 4263–4266. doi:10.1021/acs.orglett.7b01911
40. Rojas, A. J.; Zhang, C.; Vinogradova, E. V.; Buchwald, N. H.; Reilly, J.; Pentelute, B. L.; Buchwald, S. L. *Chem. Sci.* **2017,** *8,* 4257–4263. doi:10.1039/c6sc05454d
41. Lee, H. G.; Lautrette, G.; Pentelute, B. L.; Buchwald, S. L. *Angew. Chem., Int. Ed.* **2017,** *56,* 3177–3181. doi:10.1002/anie.201611202
42. Lee, H. G.; Lautrette, G.; Pentelute, B. L.; Buchwald, S. L. *Angew. Chem.* **2017,** *129,* 3225–3229. doi:10.1002/ange.201611202
43. Ma, B.; Elkayam, T.; Wolfson, H.; Nussinov, R. *Proc. Natl. Acad. Sci. U. S. A.* **2003,** *100,* 5772–5777. doi:10.1073/pnas.1030237100
44. Ruiz-Rodríguez, J.; Albericio, F.; Lavilla, R. *Chem. – Eur. J.* **2010,** *16,* 1124–1127. doi:10.1002/chem.200902676
45. Williams, T. J.; Reay, A. J.; Whitwood, A. C.; Fairlamb, I. J. S. *Chem. Commun.* **2014,** *50,* 3052–3054. doi:10.1039/c3cc48481e
46. Zhu, Y.; Bauer, M.; Ackermann, L. *Chem. – Eur. J.* **2015,** *21,* 9980–9983. doi:10.1002/chem.201501831
47. Reay, A. J.; Williams, T. J.; Fairlamb, I. J. S. *Org. Biomol. Chem.* **2015,** *13,* 8298–8309. doi:10.1039/c5ob01174d
48. Reay, A. J.; Hammarback, L. A.; Bray, J. T. W.; Sheridan, T.; Turnbull, D.; Whitwood, A. C.; Fairlamb, I. J. S. *ACS Catal.* **2017,** *7,* 5174–5179. doi:10.1021/acscatal.6b03121
49. Dong, H.; Limberakis, C.; Liras, S.; Price, D.; James, K. *Chem. Commun.* **2012,** *48,* 11644–11646. doi:10.1039/c2cc36962a
50. Mendive-Tapia, L.; Preciado, S.; García, J.; Ramón, R.; Kielland, N.; Albericio, F.; Lavilla, R. *Nat. Commun.* **2015,** *6,* 7160. doi:10.1038/ncomms8160
51. Noisier, A. F. M.; García, J.; Ionuț, I. A.; Albericio, F. *Angew. Chem., Int. Ed.* **2017,** *56,* 314–318. doi:10.1002/anie.201608648
52. Noisier, A. F. M.; García, J.; Ionuț, I. A.; Albericio, F. *Angew. Chem.* **2017,** *129,* 320–324. doi:10.1002/ange.201608648
53. Schnepel, C.; Sewald, N. *Chem. – Eur. J.* **2017,** *23,* 12064–12086. doi:10.1002/chem.201701209
54. Minges, H.; Sewald, N. *ChemCatChem* **2020,** *12,* 4450–4470. doi:10.1002/cctc.202000531
55. Dachwitz, S.; Widmann, C.; Frese, M.; Niemann, H. H.; Sewald, N. Enzymatic halogenation: enzyme mining, mechanisms, and implementation in reaction cascades. In *Amino Acids, Peptides and Proteins;* Ryadnov, M.; Hudecz, F., Eds.; Royal Society of Chemistry: Cambridge. UK, 2019; Vol. 44, pp 1–43. doi:10.1039/9781788017008-00001
56. Schnepel, C.; Minges, H.; Frese, M.; Sewald, N. *Angew. Chem., Int. Ed.* **2016,** *55,* 14159–14163. doi:10.1002/anie.201605635
57. Schnepel, C.; Minges, H.; Frese, M.; Sewald, N. *Angew. Chem.* **2016,** *128,* 14365–14369. doi:10.1002/ange.201605635
58. Frese, M.; Schnepel, C.; Minges, H.; Voß, H.; Feiner, R.; Sewald, N. *ChemCatChem* **2016,** *8,* 1799–1803. doi:10.1002/cctc.201600317
59. Gruß, H.; Belu, C.; Bernhard, L. M.; Merschel, A.; Sewald, N. *Chem. – Eur. J.* **2019,** *25,* 5880–5883. doi:10.1002/chem.201900437

60. Pubill-Ulldemolins, C.; Sharma, S. V.; Cartmell, C.; Zhao, J.; Cárdenas, P.; Goss, R. J. M. *Chem. – Eur. J.* **2019,** *25,* 10866–10875. doi:10.1002/chem.201901327
61. Sharma, S. V.; Tong, X.; Pubill-Ulldemolins, C.; Cartmell, C.; Bogosyan, E. J. A.; Rackham, E. J.; Marelli, E.; Hamed, R. B.; Goss, R. J. M. *Nat. Commun.* **2017,** *8,* 229. doi:10.1038/s41467-017-00194-3
62. Willemse, T.; Van Imp, K.; Goss, R. J. M.; Van Vlijmen, H. W. T.; Schepens, W.; Maes, B. U. W.; Ballet, S. *ChemCatChem* **2015,** *7,* 2055–2070. doi:10.1002/cctc.201500190
63. Corr, M. J.; Sharma, S. V.; Pubill-Ulldemolins, C.; Bown, R. T.; Poirot, P.; Smith, D. R. M.; Cartmell, C.; Abou Fayad, A.; Goss, R. J. M. *Chem. Sci.* **2017,** *8,* 2039–2046. doi:10.1039/c6sc04423a
64. Roy, A. D.; Grüschow, S.; Cairns, N.; Goss, R. J. M. *J. Am. Chem. Soc.* **2010,** *132,* 12243–12245. doi:10.1021/ja1060406
65. Dachwitz, S.; Duwe, D. H.; Wang, Y. H.; Gruß, H.; Hannappel, Y.; Hellweg, T.; Sewald, N. *Chem. – Eur. J.* **2020,** *26,* 16357–16364. doi:10.1002/chem.202002454
66. Gruß, H.; Sewald, N. *Chem. – Eur. J.* **2020,** *26,* 5328–5340. doi:10.1002/chem.201903756
67. Kemker, I.; Schröder, D. C.; Feiner, R. C.; Müller, K. M.; Marion, A.; Sewald, N. *J. Med. Chem.* **2021,** *64,* 586–601. doi:10.1021/acs.jmedchem.0c01536
68. Kemker, I.; Feiner, R. C.; Müller, K. M.; Sewald, N. *ChemBioChem* **2020,** *21,* 496–499. doi:10.1002/cbic.201900512
69. Ghabraie, E.; Kemker, I.; Tonali, N.; Ismail, M.; Dodero, V. I.; Sewald, N. *Chem. – Eur. J.* **2020,** *26,* 12036–12042. doi:10.1002/chem.202001312
70. Schnepel, C.; Dodero, V. I.; Sewald, N. *Chem. – Eur. J.* **2021,** *27,* 5404–5411. doi:10.1002/chem.202005191
71. García-Pindado, J.; Willemse, T.; Goss, R.; Maes, B. U. W.; Giralt, E.; Ballet, S.; Teixidó, M. *Biopolymers* **2018,** *109,* e23112. doi:10.1002/bip.23112
72. Kemker, I.; Schnepel, C.; Schröder, D. C.; Marion, A.; Sewald, N. *J. Med. Chem.* **2019,** *62,* 7417–7430. doi:10.1021/acs.jmedchem.9b00360
73. Frese, M.; Sewald, N. *Angew. Chem., Int. Ed.* **2015,** *54,* 298–301. doi:10.1002/anie.201408561
74. Frese, M.; Sewald, N. *Angew. Chem.* **2015,** *127,* 302–305. doi:10.1002/ange.201408561
75. Xing, Y.; Clements, W. K.; Kimelman, D.; Xu, W. *Genes Dev.* **2003,** *17,* 2753–2764. doi:10.1101/gad.1142603
76. Clevers, H.; Nusse, R. *Cell* **2012,** *149,* 1192–1205. doi:10.1016/j.cell.2012.05.012
77. Grossmann, T. N.; Yeh, J. T.-H.; Bowman, B. R.; Chu, Q.; Moellering, R. E.; Verdine, G. L. *Proc. Natl. Acad. Sci. U. S. A.* **2012,** *109,* 17942–17947. doi:10.1073/pnas.1208396109
78. Afonso, A.; Cussó, O.; Feliu, L.; Planas, M. *Eur. J. Org. Chem.* **2012,** 6204–6211. doi:10.1002/ejoc.201200832
79. Guan, Z.; Yates, N. A.; Bakhtiar, R. *J. Am. Soc. Mass Spectrom.* **2003,** *14,* 605–613. doi:10.1016/s1044-0305(03)00201-0
80. Afonso, A.; Feliu, L.; Planas, M. *Tetrahedron* **2011,** *67,* 2238–2245. doi:10.1016/j.tet.2011.01.084
81. Sönnichsen, F. D.; Van Eyk, J. E.; Hodges, R. S.; Sykes, B. D. *Biochemistry* **1992,** *31,* 8790–8798. doi:10.1021/bi00152a015
82. Shinohara, T.; Deng, H.; Snapper, M. L.; Hoveyda, A. H. *J. Am. Chem. Soc.* **2005,** *127,* 7334–7336. doi:10.1021/ja051790l
83. Thakkar, B. S.; Svendsen, J.-S. M.; Engh, R. A. *J. Phys. Chem. A* **2017,** *121,* 6830–6837. doi:10.1021/acs.jpca.7b05584
84. Nguyen, K.; Iskandar, M.; Rabenstein, D. L. *J. Phys. Chem. B* **2010,** *114,* 3387–3392. doi:10.1021/jp1000286
85. *AMBER18;* University of California: San Francisco, CA, USA, 2018.
86. Hamelberg, D.; Mongan, J.; McCammon, J. A. *J. Chem. Phys.* **2004,** *120,* 11919–11929. doi:10.1063/1.1755656
87. Miao, Y.; Feixas, F.; Eun, C.; McCammon, J. A. *J. Comput. Chem.* **2015,** *36,* 1536–1549. doi:10.1002/jcc.23964
88. Duan, L.; Guo, X.; Cong, Y.; Feng, G.; Li, Y.; Zhang, J. Z. H. *Front. Chem. (Lausanne, Switz.)* **2019,** *7,* 540. doi:10.3389/fchem.2019.00540
89. Kamenik, A. S.; Lessel, U.; Fuchs, J. E.; Fox, T.; Liedl, K. R. *J. Chem. Inf. Model.* **2018,** *58,* 982–992. doi:10.1021/acs.jcim.8b00097
90. Maier, J. A.; Martinez, C.; Kasavajhala, K.; Wickstrom, L.; Hauser, K. E.; Simmerling, C. *J. Chem. Theory Comput.* **2015,** *11,* 3696–3713. doi:10.1021/acs.jctc.5b00255
91. Wang, J.; Wolf, R. M.; Caldwell, J. W.; Kollman, P. A.; Case, D. A. *J. Comput. Chem.* **2004,** *25,* 1157–1174. doi:10.1002/jcc.20035
92. Sinko, W.; Miao, Y.; de Oliveira, C. A. F.; McCammon, J. A. *J. Phys. Chem. B* **2013,** *117,* 12759–12768. doi:10.1021/jp401587e
93. Miao, Y.; Sinko, W.; Pierce, L.; Bucher, D.; Walker, R. C.; McCammon, J. A. *J. Chem. Theory Comput.* **2014,** *10,* 2677–2689. doi:10.1021/ct500090q
94. Noé, F.; Rosta, E. *J. Chem. Phys.* **2019,** *151,* 190401. doi:10.1063/1.5134029
95. Toenjes, S. T.; Gustafson, J. L. *Future Med. Chem.* **2018,** *10,* 409–422. doi:10.4155/fmc-2017-0152

License and Terms

This is an open access article licensed under the terms of the Beilstein-Institut Open Access License Agreement (https://www.beilstein-journals.org/bjoc/terms), which is identical to the Creative Commons Attribution 4.0 International License (https://creativecommons.org/licenses/by/4.0). The reuse of material under this license requires that the author(s), source and license are credited. Third-party material in this article could be subject to other licenses (typically indicated in the credit line), and in this case, users are required to obtain permission from the license holder to reuse the material.

The definitive version of this article is the electronic one which can be found at:
https://doi.org/10.3762/bjoc.18.1

BEILSTEIN JOURNAL OF ORGANIC CHEMISTRY

Synthesis and late stage modifications of Cyl derivatives

Phil Servatius and Uli Kazmaier*

Full Research Paper

Open Access

Address:
Organic Chemistry, Saarland University, Campus C4.2, 66123 Saarbrücken, Germany

Email:
Uli Kazmaier* - u.kazmaier@mx.uni-saarland.de

* Corresponding author

Keywords:
chelated enolate; Claisen rearrangement; HDAC inhibitor; peptide; late stage modification

Beilstein J. Org. Chem. **2022,** *18,* 174–181.
https://doi.org/10.3762/bjoc.18.19

Received: 10 December 2021
Accepted: 24 January 2022
Published: 04 February 2022

This article is part of the thematic issue "Late-stage diversification of peptides".

Associate Editor: N. Sewald

© 2022 Servatius and Kazmaier; licensee Beilstein-Institut.
License and terms: see end of document.

Abstract

A peptide Claisen rearrangement is used as key step to generate a tetrapeptide with a C-terminal double unsaturated side chain. Activation and cyclization give direct access to cyclopeptides related to naturally occurring histone deacetylase (HDAC) inhibitors Cyl-1 and Cyl-2. Late stage modifications on the unsaturated amino acid side chain allow the introduction of functionalities which might coordinate to metal ions in the active center of metalloproteins, such as histone deacetylases.

Introduction

Among natural products, peptidic structures have entered the limelight due to their extraordinary biological activities [1]. Often found as secondary metabolites for self-defense in different microorganisms, peptidic natural products are assembled either by ribosomal synthesis or by non-ribosomal peptide synthetases (NRPS) [2]. Macrocyclic peptides are pervasive throughout this class of natural products and often show improved stability against proteolytic digest and metabolic processes [3]. Furthermore, cyclization generally helps to fix the active conformation of a peptide needed to interact with the respective cellular target. Incorporation of non-proteinogenic and unusual amino acids often is related to their biological function. For example, trapoxin B (Figure 1) is a cyclic tetrapeptide with a rather unusual epoxyketone side chain and was found to be a strong inhibitor of histone deacetylases (HDACs) [4,5].

HDACs are nuclear isozymes that regulate gene transcription via a dynamic process of acetylation and deacetylation of lysine residues of histones [6-10]. Blockade of the deacylating process causes hyperacetylation of histones and unregulated gene activity, that results in untimely cell death. Eighteen different HDAC enzymes are known so far and they are divided into four classes based on structural homology with yeast proteins [11]. Three of these enzyme classes (I, II, and IV) contain Zn^{2+} within the active site, and therefore these enzymes can be affected by typical Zn^{2+}-binding HDAC inhibitors. In cellular systems, an acetylated lysine of a histone is entering the cavity of the active site and gets coordinated to Zn^{2+}. Subsequent attack of water forms a tetrahedral intermediate which results in a cleavage of the acetylated lysine. Most HDAC inhibitors act as substrate mimics and contain a zinc-binding motif. They competitively

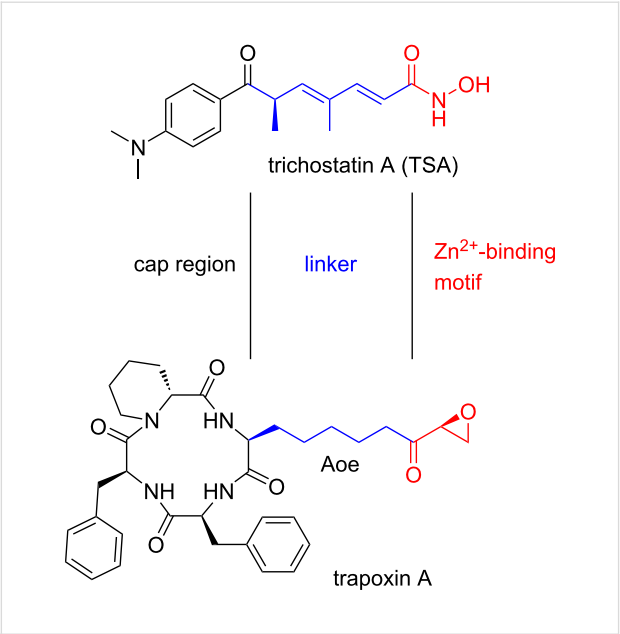


Figure 1: Naturally occurring HDAC inhibitors.

interact with the HDACs to form stable intermediates and therewith block the active site.

Many naturally occurring HDAC inhibitors are known to date [12]. Acyclic molecules like, e.g., trichostatin A (TSA, Figure 1) were among the first isolated HDAC inhibitors. Isolated in 1976 from *Streptomyces hygroscopicus* by Tsuji et al. [13], TSA played an important role in rationalizing the mode of action of HDACs [14]. Trichostatin contains a hydroxamic acid as zinc-binding motif, inspiring the design of a wide range of synthetic HDAC inhibitors. The essential Zn^{2+}-binding group is attached to a non-polar linker, delivering it inside the cavity through a narrow channel. The cap region is responsible for interactions with residues on the rim of the active site [15]. The cap region of acyclic HDAC inhibitors is generally small, resulting in non-specific interactions with the different HDAC isoforms. More diverse cap regions are found in macrocyclic HDAC inhibitors such as trapoxin which contains the unusual, non-proteinogenic amino acid (2*S*,9*S*)-2-amino-9,10-epoxy-8-oxodecanoic acid (Aoe) as a zinc-binding group.

Interestingly, Aoe with its α-epoxyketone motif is wide-spread among this compound class as it is present in other natural products such as Cyl-1 and Cyl-2 [16,17], chlamydocin [18], and many others [12]. The α-epoxyketone is isosteric to an acetylated lysine residue, which makes it a mimic of HDAC's natural substrate [10]. Although α-epoxyketones and hydroxamic acids show high affinities towards Zn^{2+}, other chelating groups are also found in natural products (Figure 2) including ketones (apicidin [19], microsporin A [20]), carboxylic acids (azumamides [21]), α-hydroxy ketones (FR235222 [22]) or thioesters (largazole [23]). These cyclopeptides mainly differ in the amino acid sequence of the peptide backbone, which causes selectivity towards the different HDAC isoforms. In fact, many naturally occurring HDAC inhibitors contain sulfur moieties like, e.g., disulfides or thioesters. They seem to lack a zinc-chelating group at first sight, but the disulfide or thioester acts as a prodrug and are reduced/cleaved in vivo to liberate the free thiol, a strong Zn-binding group [24,25].

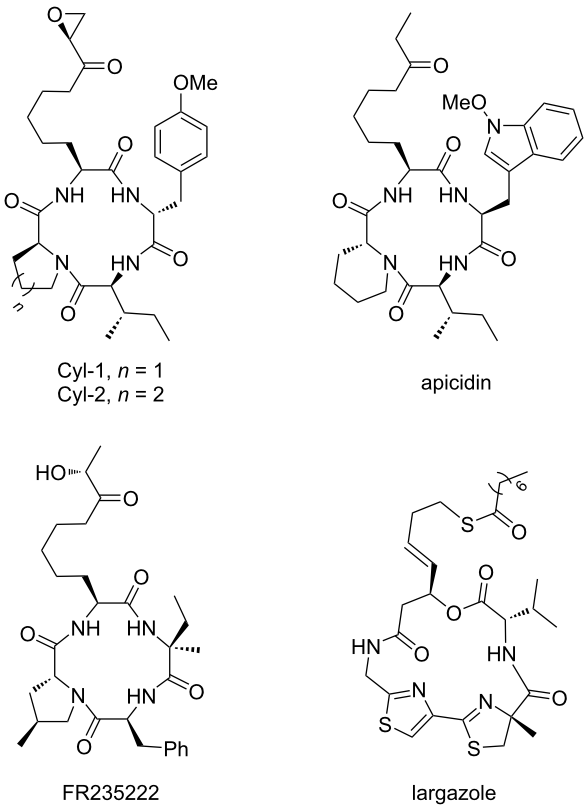


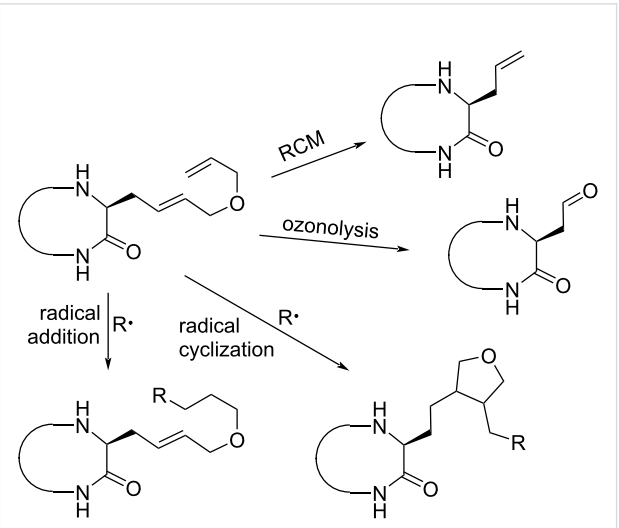
Figure 2: Naturally occurring HDAC inhibitors with different zinc-binding motifs.

Results and Discussion

Since a couple of years the focus of our research group is on the synthesis of unnatural amino acids and their incorporation into complex natural products. Many of these show interesting anticancer activities [26-28]. Some linear peptides, such as pretubulysin bind to tubulin [29-31], while others cyclodepsipeptides are strong actin binders [32,33]. Recently, we also became interested in the synthesis of the cyclic HDAC inhibitors. We developed syntheses for chlamydocin [34], Cyl-1 [35], and trapoxin [36] using either Claisen rearrangements [37,38] or Pd-catalyzed allylic alkylations [39,40] as key steps for the synthesis of the unusual Aoe, which was then incorporated into the different tetrapeptides.

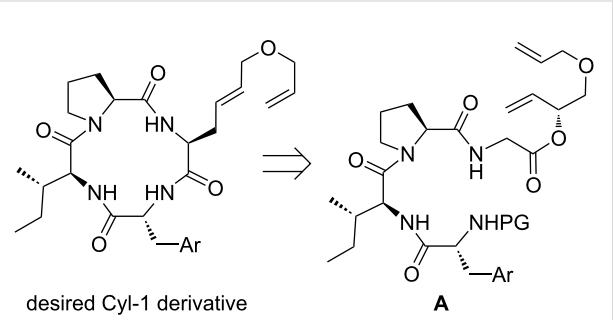
Our aim now was to develop a rather flexible protocol that allows us to introduce several types of functionalities onto a given peptide to create libraries of structurally related compounds for SAR studies. Of course, this approach is not limited to the development of HDAC inhibitors, but should be suitable for all kinds of natural product modifications. However, the structural motif of the natural products shown in Figure 2 is suitable to illustrate the concept.

In general, typical syntheses of such natural products start with the synthesis of the unusual building blocks, their incorporation into a linear peptide, which is finally subjected to cyclization at a suitable position. No question, this protocol is well suited to get access to a certain compound, also in large scale, but it is not applicable for the generation of small libraries of related compounds for SAR studies. Therefore, it is more convenient to undertake modifications at a late stage of the synthesis using a suitably modified precursor allowing variations in a straightforward manner. As a model compound, we decided to use the Cyl-1 amino acid backbone and introduce a double unsaturated side chain (Scheme 1). In principle, selective modifications at the two different double bonds (internal and terminal) should be possible. Ring-closing metathesis (RCM) should generate an allylglycine unit, which should undergo a wide range of addition reactions. Ozonolysis, on the other hand, should generate a carbonyl functionality. Radical additions towards the double unsaturated side chain of the Cyl-1 derivative might also allow cyclizations.



Scheme 1: Planned syntheses of Cyl-1 derivatives.

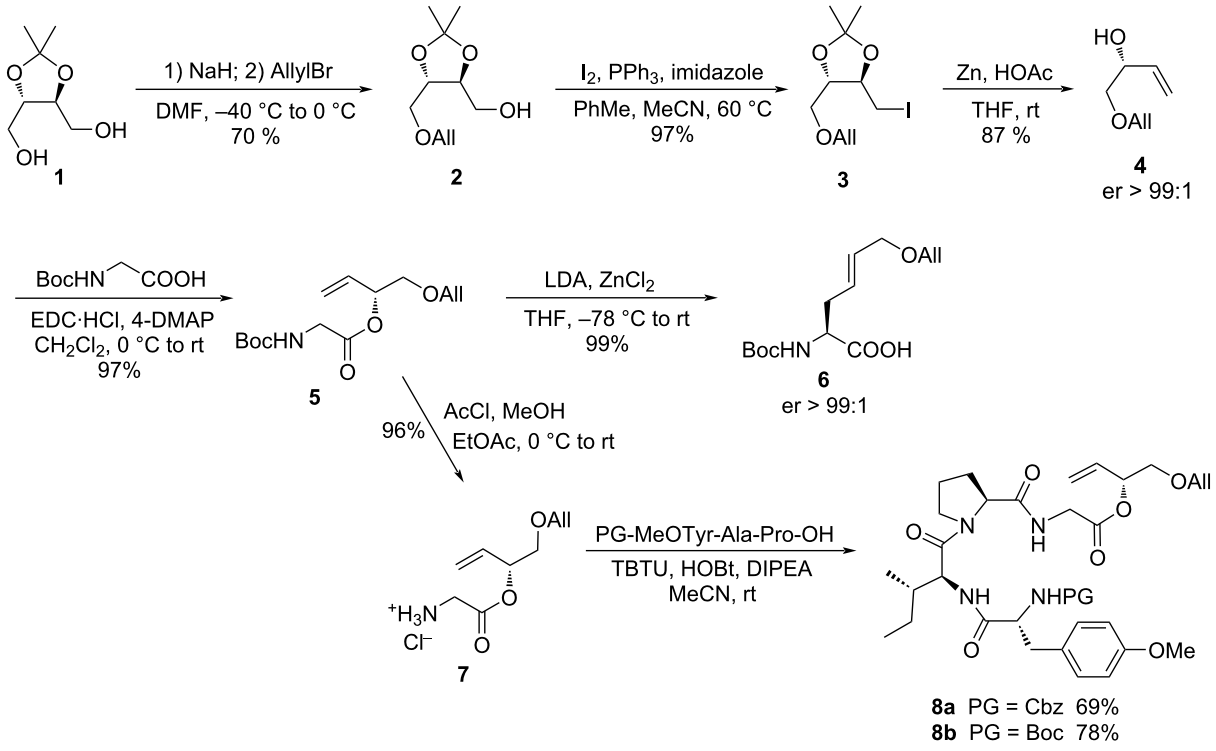
To get access to the desired double unsaturated cyclopeptide, we decided to take advantage of an asymmetric chelate enolate Claisen rearrangement, which should allow the stereoselective generation of the unusual amino acid, depending on the configuration of the chiral allylic alcohol used [41,42]. If a peptide Claisen rearrangement [43-45] is carried out with a suitable protected linear precursor **A** (Scheme 2, PG: protecting group), the resulting carboxylic acid obtained can directly be activated and subjected to cyclization. If the glycine allyl ester is incorporated as the last building block into the C-terminus of the peptide, this concept should provide a high degree of variability for the generation of small libraries, in our case of Cyl-1 derivatives.



Scheme 2: Cyl-1 derivatives via peptide Claisen rearrangement.

Chiral allylic alcohols are easily accessible, either via kinetic resolution of racemic alcohols [46,47], asymmetric catalysis [48], or from chiral pool materials, such as threitol **1** [49]. Using the last approach, **1** was mono-*O*-allylated to **2** under similar conditions reported previously for monobenzylation (Scheme 3) [50]. Iodination (**3**) and subsequent elimination of the iodide with zinc dust gave allylic alcohol **4** as a single enantiomer, which was esterified with Boc-protected glycine to allyl ester **5**. Before we incorporated this allylic ester into the desired tetrapeptide, we wanted to make sure that the chelate Claisen rearrangement does not cause any problems. And indeed, Claisen rearrangement of **5** proceeded cleanly, providing the protected amino acid **6** in almost quantitative yield and with perfect chirality transfer.

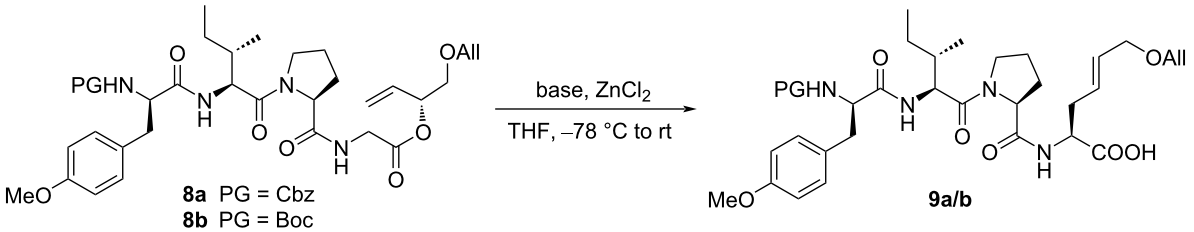
With this positive results in hand, we incorporated **5** into the desired tetrapeptide **8**. So far, we carried out peptide Claisen rearrangements only with small dipeptides, but never used longer peptide chains, such as tetrapeptides. We knew from previous work that the protecting groups on the peptide can have a significant effect on the Claisen rearrangement and therefore we synthesized the Cbz- as well as the Boc-protected peptides **8a** and **8b**. The tripeptide building blocks were previously also used in the Cyl-1 synthesis. Glycine allyl ester **5** was Boc-deprotected to give amine **7** as hydrochloride salt, using a protocol developed by Nudelman et al. [51]. Coupling with the protected tripeptides using TBTU occurred without epimerization [52].



Scheme 3: Synthesis of tetrapeptide allyl esters **8**.

The two tetrapeptide allyl esters were subjected to the peptide Claisen rearrangement, the key step of the synthesis. Subjecting allyl ester **8a** to the usual conditions of an ester enolate Claisen rearrangement with zinc chloride as chelating metal gave the rearranged product in only 33% yield and a diastereomeric ratio of 93:7 (Table 1, entry 1). The reaction was kept at −45 °C overnight to suppress potential epimerization of the peptide. Generally, epimerization is prevented through deprotonation of amide NH bonds, as argued by Seebach for Li enolates [53,54]. Nevertheless, isoleucine was prone to epimerize under the reaction conditions due to its vicinity to proline and therewith lack of the "protecting" NH group. Since no full conversion was observed in this first attempt, LDA was replaced with LHMDS and the reaction was allowed to warm to room temperature

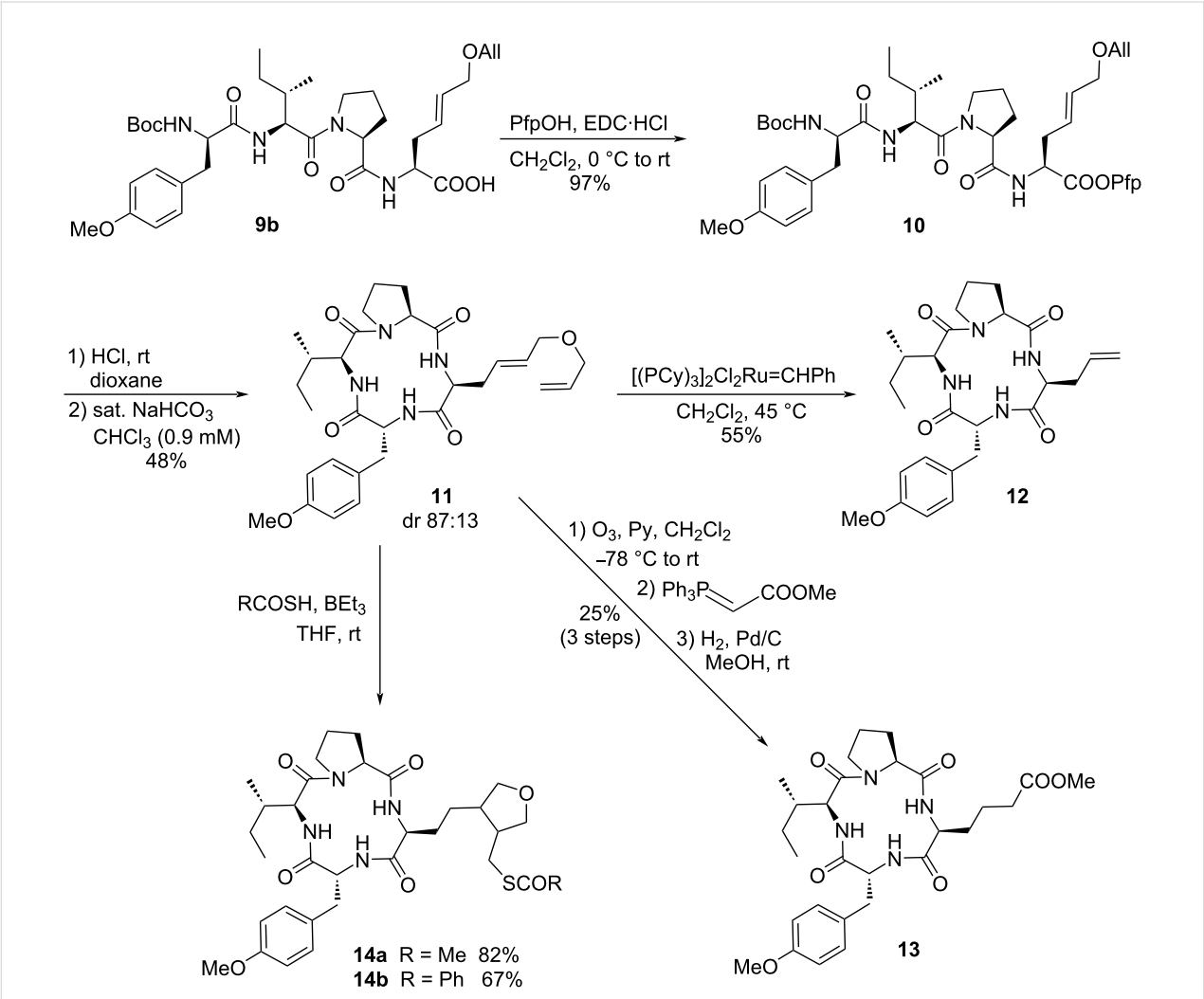
Table 1: Ester enolate Claisen rearrangements of tetrapeptide allyl esters **8**.



entry	8	base (equiv)	9	yield [%]	dr	comment
1	**8a**	LDA (4.8)	**9a**	33	93:7	no full conversion
2	**8a**	LHMDS (4.8)	**9a**	37	≈95:5	no full conversion
3	**8b**	LHMDS (4.5)	**9b**	–	–	no conversion
4	**8b**	LDA (4.5)	**9b**	34	95:5	no full conversion
5	**8b**	LDA (5.5)	**9b**	quant.	>99:1	full conversion

overnight (Table 1, entry 2). LHMDS is a weaker base than LDA and should not deprotonate α-substituted amino acid amides [53,54]. No full conversion was observed either and both yield and diastereomeric ratio were similar to the reaction with LDA. If the Boc-protected ester **8b** was then treated with LHMDS under the same reaction conditions (Table 1, entry 3) surprisingly no conversion was observed at all. Switching the base back to LDA (Table 1, entry 4) gave similar results than before (Table 1, entry 1). Since the reaction seemed to stop after 30–40% conversion, it was speculated that the ester enolate chelate complex formation was incomplete due to consumption of the base. For instance, deprotonation of tyrosine residues in benzyl position has been observed previously in the derivatization of miuraenamides and would call for an additional equivalent of base. Therefore, the reaction was repeated with 5.5 equiv LDA (Table 1, entry 5) and indeed, the desired tetrapeptide acid was obtained in quantitative yield as crude product, without obvious formation of byproducts. Strikingly, the diastereomeric ratio was also very high. Only prolonged reaction times (>18 h) led to epimerization of the rearranged peptide.

With rearranged tetrapeptide **9b** in hand, esterification with pentafluorophenol (Pfp) gave Pfp ester **10**, which should readily cyclize after Boc deprotection (Scheme 4). Treatment with HCl in dioxane gave the crude ammonium salt, which was subjected to biphasic ring closure; the hydrochloride salt was added dropwise to a stirred emulsion of saturated $NaHCO_3$ solution in chloroform [55]. Macrocycle **11** was obtained in acceptable yield as a diastereomeric mixture (dr 87:13), but the diastereomers of **11** could be separated by reversed-phase flash chromatography. It was obviously the C-terminal unusual amino acid which underwent epimerization under the reaction conditions, since already the Pfp ester **10** was partially epimerized, as deter-



Scheme 4: Synthesis and late stage modifications of Cyl derivatives.

mined later on. To access the allylglycine motif for further derivatization, pure cycle **11** was subjected to Grubbs I catalyst in dichloromethane at 45 °C to get the desired product **12**. While the reaction proceeded well even with the cyclic tetrapeptide, compound **12** proved to be highly insoluble, which complicated its purification.

An acknowledged method for the removal of metathesis catalysts is the formation of Ru-DMSO complexes, which do not eluate from a silica column [56]. This allowed us to remove at least the Ru contamination, but we were unable to subject **12** to further modifications such as cross metathesis or thiol-ene click reactions due to poor solubility. Additionally, providing sophisticated NMR spectra of **12** turned out to be a non-trivial issue. All commercially available deuterated solvents were tested as solvents and finally, recording the spectra in tetrachloroethane-d_2 at elevated temperatures (100 °C) led to a clear solution and hence clean NMR spectra.

The solubility issues forced us to investigate also other modification protocols. Thus, macrocycle **11** was subjected to an ozonolysis with subsequent Wittig reaction in a one-pot manner (Scheme 4). Performing the ozonolysis in presence of pyridine led to immediate reduction of the primary ozonide formed during the reaction [57]. Consequently, no PPh_3 or Me_2S was required to obtain the crude aldehyde. Subsequent addition of a Wittig ylide gave access to a cyclopeptide with an α,β-unsaturated ester side chain as a (*E*/*Z*) mixture. Unfortunately, this compound contained triphenylphosphine oxide as impurity, which could not be separated from the product. Subsequent hydrogenation proceeded readily and afforded the saturated cyclopeptide **13**. However, the impurity could also not be removed on this stage. Apparently, the Cyl derivatives with a short side chain are not good candidates for further modifications, mainly for solubility reasons.

Therefore, we decided to have a closer look into modifications of the longer side chain present in **11** and subjected it to thiol-ene click reactions. Since masked thiols are often found as zinc-coordinating functionalities in HDAC inhibitors, e.g., in the largazoles, we treated **11** with thioacetic acid and BEt_3/air in THF to give 82% of the thiol-ene click product (Scheme 4). Careful analysis of the NMR spectra revealed that the intermediately formed radical cyclized in an intramolecular 5-*exo*-*trig* fashion with the internal double bond to form a tetrahydrofuran cycle **14a**. The formation of the 5-membered ring system seemed to be the driving force of this reaction [58]. Comparable yields were obtained with other thiocarboxylic acids, such as thiobenzoic acid, which gave rise to the benzoylated cyclopeptide **14b**. In these cases, the obtained products were nicely soluble and could easily be purified.

Conclusion

In conclusion, we could show that chelate Claisen rearrangements can be carried out in longer peptides, such as tetrapeptides, as long as acidic positions can be identified, and the amount of base can be adjusted accordingly. The formation of thiol-ene click products **14** substantiated the hypothesis that the insolubility of Cyl derivatives with short side chains limit their synthetic applicability. The fact that **11** underwent rapid intramolecular cyclization after thiol addition renders further investigations into thiol-ene click-initiated cyclization reactions. The chain length in **14** should generally be suitable for effective HDAC inhibition and the thioester moiety might act as a prodrug as described for the natural HDAC inhibitor largazole. Further investigations are currently in progress.

Supporting Information

Supporting Information File 1

Detailed synthetic procedures, characterization of all molecules and copies of NMR spectra.
[https://www.beilstein-journals.org/bjoc/content/supplementary/1860-5397-18-19-S1.pdf]

Acknowledgements

This article is part of the PhD thesis of Phil Servatius “Total synthesis of natural HDAC inhibitors and derivatives thereof”, Saarland University, 2018.

Funding

Financial support from Saarland University is gratefully acknowledged.

ORCID® iDs

Uli Kazmaier - https://orcid.org/0000-0001-9756-0589

Preprint

A non-peer-reviewed version of this article has been previously published as a preprint: https://doi.org/10.3762/bxiv.2021.86.v1

References

1. Stolze, S. C.; Kaiser, M. *Synthesis* **2012,** *44,* 1755–1777. doi:10.1055/s-0031-1289765
2. Walsh, C. T. *Science* **2004,** *303,* 1805–1810. doi:10.1126/science.1094318
3. Sieber, S. A.; Marahiel, M. A. *Chem. Rev.* **2005,** *105,* 715–738. doi:10.1021/cr0301191
4. Itazaki, H.; Nagashima, K.; Sugita, K.; Yoshida, H.; Kawamura, Y.; Yasuda, Y.; Matsumoto, K.; Ishii, K.; Uotani, N.; Nakai, H.; Terui, A.; Yoshimatsu, S.; Ikenishi, Y.; Nakagawa, Y. *J. Antibiot.* **1990,** *43,* 1524–1532. doi:10.7164/antibiotics.43.1524

5. Mwakwari, S. C.; Patil, V.; Guerrant, W.; Oyelere, A. K. *Curr. Top. Med. Chem.* **2010,** *10,* 1423–1440. doi:10.2174/156802610792232079
6. Wolffe, A. P. *Science* **1996,** *272,* 371–372. doi:10.1126/science.272.5260.371
7. Pazin, M. J.; Kadonaga, J. T. *Cell* **1997,** *89,* 325–328. doi:10.1016/s0092-8674(00)80211-1
8. Hassig, C. A.; Tong, J. K.; Fleischer, T. C.; Owa, T.; Grable, P. G.; Ayer, D. E.; Schreiber, S. L. *Proc. Natl. Acad. Sci. U. S. A.* **1998,** *95,* 3519–3524. doi:10.1073/pnas.95.7.3519
9. Grozinger, C. M.; Schreiber, S. L. *Proc. Natl. Acad. Sci. U. S. A.* **2000,** *97,* 7835–7840. doi:10.1073/pnas.140199597
10. Meinke, P. T.; Liberator, P. *Curr. Med. Chem.* **2001,** *8,* 211–235. doi:10.2174/0929867013373787
11. Marks, P. A.; Breslow, R. *Nat. Biotechnol.* **2007,** *25,* 84–90. doi:10.1038/nbt1272
12. Maolanon, A. R.; Kristensen, H. M. E.; Leman, L. J.; Ghadiri, M. R.; Olsen, C. A. *ChemBioChem* **2017,** *18,* 5–49. doi:10.1002/cbic.201600519
13. Tsuji, N.; Kobayashi, M.; Nagashima, K.; Wakisaka, Y.; Koizumi, K. *J. Antibiot.* **1976,** *29,* 1–6. doi:10.7164/antibiotics.29.1
14. Finnin, M. S.; Donigian, J. R.; Cohen, A.; Richon, V. M.; Rifkind, R. A.; Marks, P. A.; Breslow, R.; Pavletich, N. P. *Nature* **1999,** *401,* 188–193. doi:10.1038/43710
15. Miller, T. A.; Witter, D. J.; Belvedere, S. *J. Med. Chem.* **2003,** *46,* 5097–5116. doi:10.1021/jm0303094
16. Hirota, A.; Suzuki, A.; Suzuki, H.; Tamura, S. *Agric. Biol. Chem.* **1973,** *37,* 643–647. doi:10.1080/00021369.1973.10860699
17. Takayama, S.; Isogai, A.; Nakata, M.; Suzuki, H.; Suzuki, A. *Agric. Biol. Chem.* **1984,** *48,* 839–842. doi:10.1080/00021369.1984.10866232
18. Closse, A.; Huguenin, R. *Helv. Chim. Acta* **1974,** *57,* 533–545. doi:10.1002/hlca.19740570306
19. Singh, S. B.; Zink, D. L.; Polishook, J. D.; Dombrowski, A. W.; Darkin-Rattray, S. J.; Schmatz, D. M.; Goetz, M. A. *Tetrahedron Lett.* **1996,** *37,* 8077–8080. doi:10.1016/0040-4039(96)01844-8
20. Gu, W.; Cueto, M.; Jensen, P. R.; Fenical, W.; Silverman, R. B. *Tetrahedron* **2007,** *63,* 6535–6541. doi:10.1016/j.tet.2007.04.025
21. Nakao, Y.; Yoshida, S.; Matsunaga, S.; Shindoh, N.; Terada, Y.; Nagai, K.; Yamashita, J. K.; Ganesan, A.; van Soest, R. W. M.; Fusetani, N. *Angew. Chem., Int. Ed.* **2006,** *45,* 7553–7557. doi:10.1002/anie.200602047
Angew. Chem. **2006**, *118,* 7715–7719. doi:10.1002/ange.200602047
22. Mori, H.; Urano, Y.; Kinoshita, T.; Yoshimura, S.; Takase, S.; Hino, M. *J. Antibiot.* **2003,** *56,* 181–185. doi:10.7164/antibiotics.56.181
23. Taori, K.; Paul, V. J.; Luesch, H. *J. Am. Chem. Soc.* **2008,** *130,* 1806–1807. doi:10.1021/ja7110064
24. Xiao, J. J.; Byrd, J.; Marcucci, G.; Grever, M.; Chan, K. K. *Rapid Commun. Mass Spectrom.* **2003,** *17,* 757–766. doi:10.1002/rcm.976
25. Furumai, R.; Matsuyama, A.; Kobashi, N.; Lee, K.-H.; Nishiyama, M.; Nakajima, H.; Tanaka, A.; Komatsu, Y.; Nishino, N.; Yoshida, M.; Horinouchi, S. *Cancer Res.* **2002,** *62,* 4916–4921.
26. Gorges, J.; Kazmaier, U. *Org. Lett.* **2018,** *20,* 2033–2036. doi:10.1021/acs.orglett.8b00576
27. Servatius, P.; Stach, T.; Kazmaier, U. *Eur. J. Org. Chem.* **2019,** 3163–3168. doi:10.1002/ejoc.201900460
28. Andler, O.; Kazmaier, U. *Org. Biomol. Chem.* **2021,** *19,* 4866–4870. doi:10.1039/d1ob00713k
29. Ullrich, A.; Chai, Y.; Pistorius, D.; Elnakady, Y. A.; Herrmann, J. E.; Weissman, K. J.; Kazmaier, U.; Müller, R. *Angew. Chem., Int. Ed.* **2009,** *48,* 4422–4425. doi:10.1002/anie.200900406
30. Ullrich, A.; Herrmann, J.; Müller, R.; Kazmaier, U. *Eur. J. Org. Chem.* **2009,** 6367–6378. doi:10.1002/ejoc.200900999
31. Hoffmann, J.; Gorges, J.; Junk, L.; Kazmaier, U. *Org. Biomol. Chem.* **2015,** *13,* 6010–6020. doi:10.1039/c5ob00587f
32. Karmann, L.; Schultz, K.; Herrmann, J.; Müller, R.; Kazmaier, U. *Angew. Chem., Int. Ed.* **2015,** *54,* 4502–4507. doi:10.1002/anie.201411212
33. Becker, D.; Kazmaier, U. *Eur. J. Org. Chem.* **2015,** 2591–2602. doi:10.1002/ejoc.201403577
34. Quirin, C.; Kazmaier, U. *Eur. J. Org. Chem.* **2009,** 371–377. doi:10.1002/ejoc.200800890
35. Servatius, P.; Kazmaier, U. *Org. Biomol. Chem.* **2018,** *16,* 3464–3472. doi:10.1039/c8ob00391b
36. Servatius, P.; Kazmaier, U. *J. Org. Chem.* **2018,** *83,* 11341–11349. doi:10.1021/acs.joc.8b01569
37. Kazmaier, U.; Maier, S. *Tetrahedron* **1996,** *52,* 941–954. doi:10.1016/0040-4020(95)00946-9
38. Kazmaier, U.; Schneider, C. *Synlett* **1996,** 975–977. doi:10.1055/s-1996-5637
39. Kazmaier, U.; Pohlman, M. *Synlett* **2004,** 623–626. doi:10.1055/s-2004-817776
40. Kazmaier, U. *Org. Chem. Front.* **2016,** *3,* 1541–1560. doi:10.1039/c6qo00192k
41. Kazmaier, U.; Schneider, C. *Tetrahedron Lett.* **1998,** *39,* 817–818. doi:10.1016/s0040-4039(97)10855-3
42. Kazmaier, U.; Schneider, C. *Synthesis* **1998,** 1321–1326. doi:10.1055/s-1998-6104
43. Kazmaier, U.; Maier, S. *J. Org. Chem.* **1999,** *64,* 4574–4575. doi:10.1021/jo9904821
44. Kazmaier, U.; Maier, S. *Org. Lett.* **1999,** *1,* 1763–1766. doi:10.1021/ol9910262
45. Maier, S.; Kazmaier, U. *Eur. J. Org. Chem.* **2000,** 1241–1251. doi:10.1002/1099-0690(200004)2000:7<1241::aid-ejoc1241>3.0.co;2-u
46. Johnson, R. A.; Sharpless, K. B. Catalytic Asymmetric Epoxidation of Allylic Alcohols. In *Catalytic Asymmetric Synthesis;* Ojima, I., Ed.; VCH: New York, NY, USA, 1993; p 103.
47. Gais, H.-J. Hydrolysis and formation of C-O-bonds. In *Enzyme Catalysis in Organic Synthesis;* Drauz, K.; Waldmann, H., Eds.; Wiley-VCH: Weinheim, Germany, 1995; p 178.
48. Lumbroso, M. A.; Cooke, M. L.; Breit, B. *Angew. Chem., Int. Ed.* **2013,** *52,* 1890–1932. doi:10.1002/anie.201204579
Angew. Chem. **2013,** *125,* 1942–1986. doi:10.1002/ange.201204579
49. Schneider, C.; Kazmaier, U. *Synthesis* **1998,** 1314–1320. doi:10.1055/s-1998-6103
50. Hungerbühler, E.; Seebach, D. *Helv. Chim. Acta* **1981,** *64,* 687–702. doi:10.1002/hlca.19810640311
51. Nudelman, A.; Bechor, Y.; Falb, E.; Fischer, B.; Wexler, B. A.; Nudelman, A. *Synth. Commun.* **1998,** *28,* 471–474. doi:10.1080/00397919808005101
52. Ivanov, A. S.; Zhalnina, A. A.; Shishkov, S. V. *Tetrahedron* **2009,** *65,* 7105–7108. doi:10.1016/j.tet.2009.06.042
53. Seebach, D. *Angew. Chem., Int. Ed. Engl.* **1988,** *27,* 1624–1654. doi:10.1002/anie.198816241
Angew. Chem. **1988, 100,** 1685–1715. doi:10.1002/ange.19881001206
54. Seebach, D. *Aldrichimica Acta* **1992,** *25,* 59–66.
55. Schmidt, U.; Weller, D.; Holder, A.; Lieberknecht, A. *Tetrahedron Lett.* **1988,** *29,* 3227–3230. doi:10.1016/0040-4039(88)85128-1

56. Ahn, Y. M.; Yang, K.; Georg, G. I. *Org. Lett.* **2001,** *3,* 1411–1413. doi:10.1021/ol010045k
57. Willand-Charnley, R.; Dussault, P. H. *J. Org. Chem.* **2013,** *78,* 42–47. doi:10.1021/jo3015775
58. Beckwith, A. L. J.; Schiesser, C. H. *Tetrahedron* **1985,** *41,* 3925–3941. doi:10.1016/s0040-4020(01)97174-1

License and Terms

This is an open access article licensed under the terms of the Beilstein-Institut Open Access License Agreement (https://www.beilstein-journals.org/bjoc/terms), which is identical to the Creative Commons Attribution 4.0 International License (https://creativecommons.org/licenses/by/4.0). The reuse of material under this license requires that the author(s), source and license are credited. Third-party material in this article could be subject to other licenses (typically indicated in the credit line), and in this case, users are required to obtain permission from the license holder to reuse the material.

The definitive version of this article is the electronic one which can be found at:
https://doi.org/10.3762/bjoc.18.19